JOURNAL OF CATALYSIS **158,** 142–169 (1996)
ARTICLE NO. 0015

Study of the Preparation of Bulk Powder Tungsten Carbides by Temperature Programmed Reaction with $CH_4 + H_2$ Mixtures

G. Leclercq,* M. Kamal,* J. M. Giraudon,* P. Devassine,* L. Feigenbaum,* L. Leclercq,* A. Frennet,† J. M. Bastin,† A. Löfberg,† S. Decker,† and M. Dufour†

**Laboratoire de Catalyse Hétérogène et Homogène, URA CNRS 402, Université des Sciences et Technologies de Lille, 59655 Villeneuve d'Ascq Cedex, France; and †Catalyse Hétérogène CP 243, Université Libre de Bruxelles, 1050 Bruxelles, Belgium*

Received February 24, 1994; revised July 26, 1995; accepted August 25, 1995

The synthesis of bulk tungsten carbides by carburization of W metal or of WO_3 with mixtures of CH_4 in hydrogen at various pressures has been studied in temperature programmed experiments. The resulting solids have been characterized by elemental analysis, X-ray diffraction, XPS analysis, and specific surface area measurements. The carburization occurs in two distinct steps: W_2C is formed in the first step taking place at about 650°C at atmospheric pressure with a 20% CH_4–H_2 mixture, while the formation of WC occurs only at higher temperatures. During carburization some free carbon is deposited, the importance of which is very much dependent on CH_4 partial pressure and on the temperature of carburization. It has also been shown that direct carburization of WO_3 by CH_4–H_2 does not take place, but that the carburization occurs via the reduction of WO_3 to W metal. The rate of reduction of WO_3 and that of carburization of W metal are very much dependent on, respectively, hydrogen partial pressure and CH_4 partial pressure. The extent of reduction of WO_3 into W metal required for carburization which takes place also depends on CH_4 partial pressure, indicating a competition between carburization of W metal at the surface and diffusion of W metal into the bulk of the solid. © 1996 Academic Press, Inc.

INTRODUCTION

Transition metal carbides are expected to gain wide application due to their unusual properties (1), in particular in catalysis. Their effectiveness as catalysts was demonstrated 20 years ago. For example, tungsten carbide was shown to exhibit an interesting catalytic behavior in reactions catalyzed by noble metals such as Pt and Pd (2). Other investigations (3–5) have since tried to explore the suitability of using highly dispersed tungsten carbides as inexpensive alternative catalysts to Pt or other noble metals in reactions such as hydrocarbon reforming (6–8) and hydrogenation of alkenes (4), and in the electro-oxidation of hydrogen or methanol in fuel cells (9, 10).

For a binary alloy such as WC, which is a rather complex heterogeneous catalyst, crucial synthesis experiments are needed to identify the factors which are of importance in controlling the surface composition and in particular the surface carbon and amount of oxygen impurity. Two experimental approaches can be defined to solve this problem:

(i) Synthesis of high purity bulk powder tungsten carbide catalysts. The aim here is to obtain well-defined structures with precisely-known surface compositions and with reasonable surface areas of a few square meters per gram.

(ii) Synthesis of bulk carbides with high specific surface areas and porous textures suitable for catalysis. These characteristics are often accompanied by lower purity of samples, suited for studying the effects of surface oxygen and excess carbon on the catalytic properties.

We have mainly focused our research work on the first approach (11). The second approach has been extensively used by Boudart and his group, who have achieved meaningful results on catalysts with specific surface areas between 50 and 200 $m^2\ g^{-1}$ (12–14).

Various methods of preparing transition metal carbides are listed in Table 1. In this paper, we have chosen to investigate in detail the preparation steps of tungsten carbide from tungsten metal and tungsten trioxide, using CH_4 as carbiding agent in a mixture with hydrogen. CH_4 has been chosen as carbiding agent in order to reduce as much as possible the formation of carbon deposits at the surface of the carbide. It is well known that methane is the least reactive of the alkanes, and accordingly requires the highest temperature for reaction, conditions where diffusion of carbon in the solid is no longer the rate limiting step.

The objective of this paper is to optimize the conditions of the preparation of tungsten carbides by varying the total pressure, the ratio of the reactants, and the temperature of carburization.

EXPERIMENTAL

Tungsten Precursors

The precursors containing tungsten used in this study were either WO_3 (Fluka, high purity grade 99.9%, BET

0021-9517/96 $12.00

TABLE 1

General Methods of Synthesis of Transition Metal Carbides

Preparation method	Reaction	References
A. Solid–solid reaction		
(1) Direct reaction of metal or metal hydride with carbon black	$x\mathrm{Me} + y\mathrm{C} \xrightarrow[1800^\circ\mathrm{C}]{} \mathrm{Me}_x\mathrm{C}_y$	(1, 3, 11, 15)
(2) Direct reaction of metal oxide and carbon black	$\mathrm{MeO} + \mathrm{C} \rightarrow \mathrm{MeC} + \mathrm{CO}$	(1, 3, 11, 15)
B. Solid–gas reaction		
(1) Reaction of metal or oxide with carbiding reagents	—disproportionation of CO	
	$\mathrm{Me} + \mathrm{CO} \rightarrow \mathrm{MeC} + \mathrm{CO_2}$	(11)
	$\mathrm{MeO} + \mathrm{CO} \rightarrow \mathrm{MeC} + \mathrm{CO_2}$	(16, 17)
	—with $CO–CO_2$ and $CO–H_2$ mixtures	
	—with hydrocarbons	(11)
	$\mathrm{Me} + \mathrm{C}_x\mathrm{H}_y \rightarrow \mathrm{MeC} + \mathrm{H_2}$	(18, 19)
	$\mathrm{MeO} + \mathrm{C}_x\mathrm{H}_y \rightarrow \mathrm{MeC} + \mathrm{CO} + \mathrm{H_2O}$	(12–14)
	—$CH_4–H_2$ mixtures	
(2) Reaction of metal nitride with $CH_4–H_2$ mixtures	Ex. $\beta\mathrm{W_2N} \rightarrow \beta\mathrm{W_2C}$	(6)
(3) Pyrolysis of an organometallic complex under hydrogen	Ex. 1 $Cp_2W_2(CO)_4$(dmad)[a]	(20)
	Ex. 2 $Cp_2Mo_2(CO)_4$(dmad)	(21)
C. Gas–gas reaction		
(1) Reaction of metal chloride or metal carbonyl with hydrocarbons, hydrogen, or CO by chemical vapor deposition	$\mathrm{WCl_6} + \mathrm{C}_x\mathrm{H}_y + \mathrm{H_2} \rightarrow \mathrm{WC} + \mathrm{HCl} + \mathrm{C}_m\mathrm{H}_n$ $\mathrm{Mo(CO)_6} + \mathrm{CO}\ (\text{or } \mathrm{H_2}) \rightarrow \mathrm{Mo_2C} + \mathrm{CO} + \mathrm{CO_2} + \mathrm{H_2O}$	(15)
(2) Reaction of metal oxide vapor with gasified carbon (under vacuum)	$\mathrm{WO_2} + 3\mathrm{C} \rightarrow \mathrm{WC} + 2\mathrm{CO}$ $2\mathrm{MoO_3} + 7\mathrm{C} \rightarrow \mathrm{Mo_2C} + 6\mathrm{CO}$	(22, 23)

[a] Cp is cyclopentadienyl and dmad is dimethylacetylenedicarboxylate.

surface area about 3 $m^2\ g^{-1}$, mixture of monoclinic and orthorombic crystallographic phases) or WO_3 prepared in our laboratory by ammonium metatungstate ($(NH_4)_6H_2W_{12}O_{40}$, xH_2O, Fluka, high purity grade 97%) decomposition (24).

Surface and Bulk Characterization

X-ray diffraction. The bulk structure of the materials was determined by X-ray diffraction using either a Philips (Norelco PW 1051) apparatus (Cu$K\alpha$ radiation $\lambda = 1.54178$ Å, Ni filter) or a diffractometer (Siemens D 5000) equipped with a specially designed *in situ* X-ray diffraction cell. A chosen gas mixture was passed through the platinum cell while the XRD patterns were collected using the diffractometer. These XRD patterns were assigned using the JCPDS data base (Joint Committee on Powder Diffraction Standards).

Chemical analysis. Elemental analyses were performed at the "Service Central de Microanalyse" of the CNRS (Vernaison, France) by coulometry for C and O, and by plasma emission spectroscopy for W after fusion of the samples in NaOH + KNO_3.

Surface areas. Surface areas were measured with a sorptometer (Quantasorb Jr.), using the single point BET surface area determination. Samples (200 to 300 mg) were placed in a cell and heated with nitrogen to 150°C. After outgassing, the cell was cooled to room temperature, then to −196°C in liquid nitrogen. The sample was then submitted to a mixture N_2 (30%)–He, and the cell was warmed to room temperature. The amount of nitrogen desorbed was measured with a thermoconductivity detector.

X-ray photoelectron spectroscopy. XPS measurements were carried out with an AEI ES 200B (Bruker) spectrometer equipped with an Al anode ($h\nu = 1486.6$ eV, 300 W). The binding energies (BE) were determined using the C 1*s* peak of contamination (BE = 285 eV) as a reference.

Reduction and Carburization of the Precursors

Two different setups were used for reduction experiments.

Temperature programmed reduction. The first setup (called apparatus TPR hereafter) employed a TCD as detector for hydrogen in a flow of H_2–Ar mixture which contained initially 30% H_2. First the sample (about 60 mg of WO_3) was dried in a flow of nitrogen at 500°C for a few hours and cooled to room temperature. Then nitrogen was replaced by the reducing mixture (flow rate 2.6 liter h^{-1}). Water formed during reduction was trapped by a 13X molecular sieve at −196°C. The data from the thermocouple and from the TCD were collected and processed by a Hewlett Packard HP 85 microcomputer.

Thermogravimetry (*TPG*). The second setup employed an electronic microbalance (Sartorius GmbH) to follow the weight loss when samples were heated (60°C h^{-1}) in vacuum (10^{-6} Torr with an oil diffusion pump). (1 Torr = 133.3 N m^{-2}.)

Preparation of Carbides by Temperature Programmed (TP) Experiments

Three different systems were used according to the total pressure requirements, and will be referred to as APR1, APR2, and LPR. Two of them were operated at atmospheric pressure (APR1 and APR2) and the third at lower pressures (LPR).

Atmospheric pressure reactor No. 1 (APR1). This reactor, located at Villeneuve d'Ascq, was a flow reactor, which was used previously in catalytic studies (25). For the present carburization experiments, the flow rates were regulated by membrane flow regulators (Brookes 8802) and measured by soap bubble flowmeters. The reactor was about 10-cm long and 2-cm wide. A thermocouple well made it possible for the temperature of the sample to be measured. The size of the sample was usually around 3 g of WO_3, but, in some cases, was up to 12 g. The gas flow rate of the carburizing mixture was about 8–10 liter h^{-1}. The heating rate in the TP experiments was 50°C h^{-1}. When reduction preceded carburization it was carried out at 600°C for 10 h after heating from room temperature at a rate of 50°C h^{-1}. Before each experiment the sample was pretreated in a nitrogen flow (about 10 liter h^{-1}) at 550°C and then cooled to room temperature. After carburization the sample was cooled to room temperature in the CH_4–H_2 mixture (unless mentioned otherwise), swept by a nitrogen flow (10 liter h^{-1}) until no hydrogen was detected by chromatography, and finally passivated in an O_2–N_2 mixture (1.5% O_2) at a flow rate of 10 liter h^{-1} for at least 10 h in order to avoid bulk oxidation when the carbide was contacted with air.

The composition of the gas mixture at the outlet of the reactor was periodically measured by gas chromatography using a Shimadzu chromatograph GC9A equipped with both TCD and flame ionization detectors (FID). Products were separated at 90°C in a column (3-m long and 1/8-inch wide) filled with "Carbosphere" molecular sieve. Peak areas were measured with an integrator (Spectra Physics 4270).

Hydrogen (Air Liquide—U quality) was purified by flowing through a Pd catalyst (Deoxo) and through a 13X molecular sieve. Air (Air Liquide) was purified by a 13X molecular sieve and nitrogen (Air Liquide—U quality) was passed through copper heated at 300°C in order to remove oxygen, and then through a 13X molecular sieve. Methane (Air Liquide—N 30 quality, 99.9%) was purified by passing through a 4A molecular sieve.

Atmospheric pressure reactor No. 2 (APR2). This apparatus, located in Brussels, was a classical flow reactor working at atmospheric pressure with partial pressures of reactive gases ranging from 0.02 to 0.3 atm and argon as balance gas. The analysis of the gas composition at the outlet of the reactor was performed by a quadrupole mass spectrometer (QMG-420-5 from Balzers) equipped with a GEV-010 (Balzers) inlet device. Gas flow rates were measured and regulated by Rosemount Sho-Rate 150 flowmeters equipped with needle valves. Typical flow rates ranged from 1.2 to 5 liter h^{-1}. A Eurotherm 818 controller using chromel-alumel thermocouples was used for measuring and controlling the reactor temperature.

Quadstar 3.0 software (Balzers) running on an IBM-type computer was used for controlling the mass spectrometer and for collecting temperature data. Samples of 40 to 150 mg of WO_3 were placed in a quartz reactor (volume 1–3 ml) connected to the apparatus through Cajon adaptors. They were then purged in pure argon at room temperature until the mass signals typical of air had returned to the baseline. The sample was then dried at 500°C in flowing argon. Meanwhile the mixture of the reactants (CH_4 and hydrogen) was prepared in the bypass. After cooling the sample to room temperature, this mixture was switched to the reactor and, after a few minutes, the temperature programming was started (typically a linear ramp of 180 to 360°C h^{-1}).

The gases used in this apparatus were argon N 50, 10.0% H_2 in argon "certified standard," 10.0% CH_4 in argon "certified standard" from UCAR, and 10.0% O_2 in argon "alpha standard" from BOC for experiments in argon or with reactant pressure lower than 0.1 atm. Pure hydrogen (N 50 from BOC) diluted in argon was used for hydrogen partial pressures between 0.1 and 0.23 atm.

Low pressure reactor (LPR). The following experiments were performed on this apparatus which was located in Brussels.

(i) Determination of total surface areas, obtained through krypton adsorption measurements and evaluation using the BET and Kaganer (26) equations. It has been shown (27) that, when applied in their respective appropriate coverage ranges, these two methods provide values in excellent agreement.

(ii) Reduction or carburization reactions in temperature programmed conditions with total pressures lower than 10 Torr.

The reaction vessel was built completely of commercial stainless steel elements, connected through 2.75 inch Conflant flanges, with the exception of the reactor itself (made of quartz) and the copper and Viton seals and gaskets. The high vacuum in this reaction vessel was obtained through an oil diffusion pump, while an ion pump enabled the sample to be kept at pressure below 10^{-8} Torr between different experiments. The pressure was measured during experiments by a membrane capacitance micromanometer

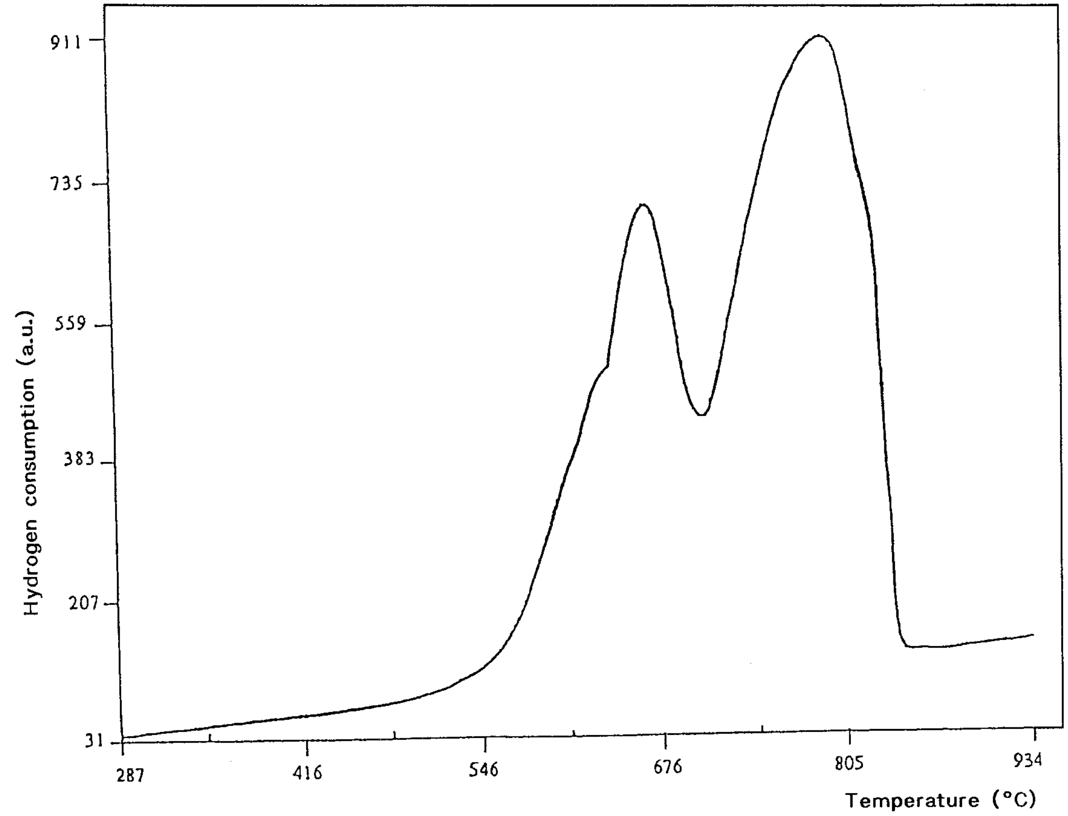

FIG. 1. TPR of WO_3 in 30% H_2–Ar (300°C h^{-1}, 64 mg). TCD signal (in arbitrary units) versus temperature.

(Barocel from Datametric) within the range 10^{-4} to 10 Torr, the UHV pressure when working with the ion pump was measured with a VG Bayard-Alpert gauge.

The introduction of gases into the apparatus was controlled by two Phillips-Granville "type C ultra-high vacuum" valves while the outlet flow rate was determined by fritted disks. The apparatus was equipped with two such fritted disks, each of them having different values of volume flow rate (14 and 55 ml s^{-1} for H_2). The advantage of working with these fritted disks is that in the whole working pressure range (10^{-4} to 10 Torr) their volume flow rate is only dependent on the nature of the flowing molecules and is independent of the pressure (molecular flow conditions). A LMD 100 manipulator (VG) allowed the insertion of the most appropriate fritted disk for the experiment.

During experiments conducted in flow conditions the nature of the gaseous molecules could be determined using a GD 150 mass spectrometer from Atlas Werk.

The gases used were the following: H_2 N 55 and Kr N 45 from BOC, and D_2 N 28, O_2 N 50, and CH_4 N 55 from UCAR.

A sample of 74 mg WO_3 (Fluka) was calcined in a flow of oxygen at 8 Torr from 25 to 1000°C. Then, after cooling, it was submitted to a flow of a 20% CH_4–D_2 mixture at 5 or 0.5 Torr at a heating rate of 360°C h^{-1} from 25 to 1200°C, where it was left at 1200°C for 35 min. During this experiment the peaks at mass 2, 3, 12, 15 to 20, 28, and 44 were recorded at various times of reaction.

RESULTS AND DISCUSSION

1. Reduction of Tungsten Trioxide

1.1. Reduction by Hydrogen at a Pressure of 0.3 atm

In a first experiment, TPR (300°C) of WO_3 (Fluka, 64 mg) was studied in apparatus TPR in a H_2 (30%)–Ar flow (2.6 liter h^{-1}) at atmospheric pressure. The variation of H_2 consumption, as measured by the TCD signal, as a function of the temperature (Fig. 1) shows that the reduction of WO_3 into W takes place in at least three steps. The hydrogen consumption starts at about 480°C, then there is a shoulder at about 640°C which may indicate the formation of a metastable oxidic form of stoichiometry between WO_3 and WO_2. The hydrogen consumption for this shoulder is about 9.3% of the total consumption which would correspond to the reduction of WO_3 into $W_{18}O_{49}$ or $W_{20}O_{58}$,

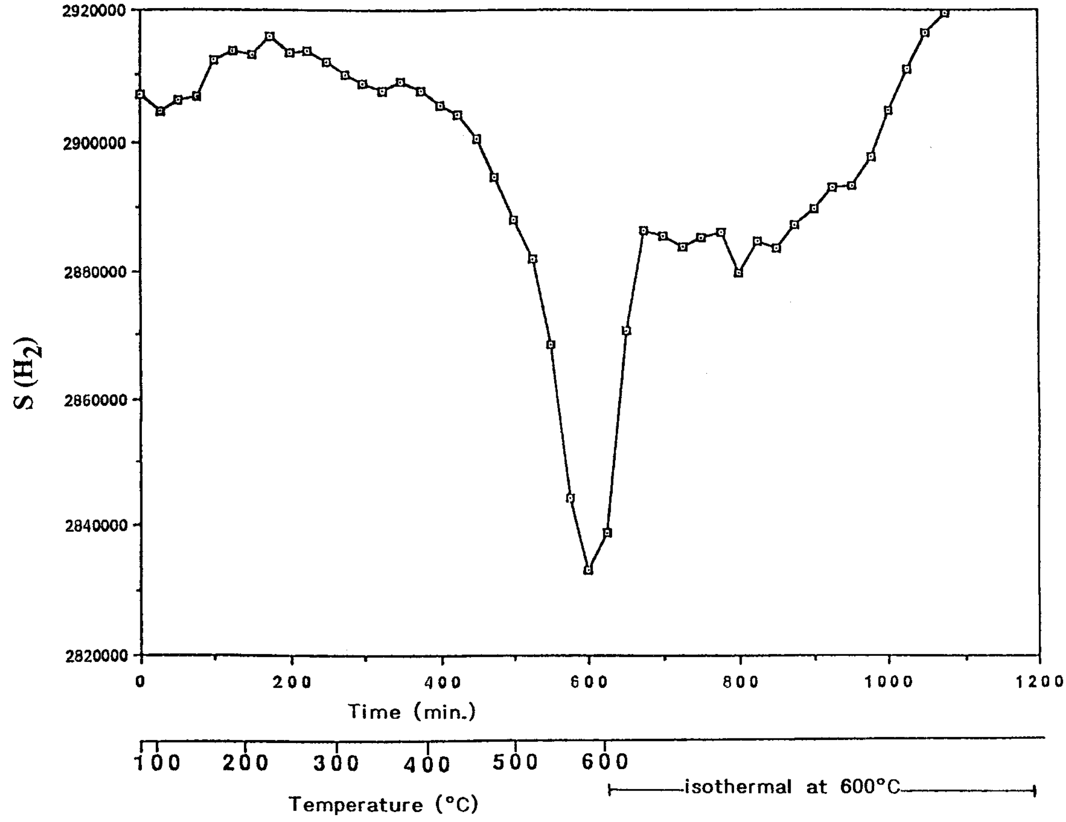

FIG. 2. Reduction of WO_3 in pure H_2 at atmospheric pressure. Area of H_2 chromatographic peak versus time. Heated at 50°C h^{-1} up to 600°C, then at constant temperature. $m = 3.05$ g.

the formation of which has already been reported (28). A first maximum of hydrogen consumption is observed at about 670°C. The uptake made up of these two features (640 and 670°C) is about one half of that of the second peak at 800°C. Hence the first peak probably corresponds to the formation of WO_2. In the final step which starts at about 710°C and leads to the second peak, the maximum reduction rate being at 800°C, WO_2 is reduced into W metal. These results are in good qualitative agreement with those of Vermaire and van Berge (29) and of Grünert *et al.* (30) who, when studying the reduction of WO_3 by XPS, have shown that it proceeds through intermediate oxidation states W^{5+}, W^{4+}, W^{2+}, and finally W^0.

1.2. Reduction by Hydrogen at a Pressure of 1 atm (Apparatus APR1)

The above study has shown that, under our conditions of TPR, WO_3 is completely reduced by hydrogen at 850°C. However, at such a temperature W metal is likely to be severely sintered. Consequently, we have checked whether WO_3 could be completely reduced in pure hydrogen at atmospheric pressure in the flow reactor used for carburization (APR1). A sample of WO_3 (Fluka, 1.32×10^{-2} mol), after drying at 550°C in a flow of nitrogen, was heated in a flow of hydrogen (9.6 liter h^{-1}) up to 600°C where it stayed for 10 h. The composition of the gas flowing out of the reactor was determined by GC in order to follow the variations of the hydrogen partial pressure (which is proportional to the area of the hydrogen peaks in GC). Figure 2 shows the result. It is not possible to determine precisely when hydrogen starts to be consumed, but certainly it is being consumed at 400°C. Hence, under 1 atm of hydrogen, the temperature where WO_3 reduction starts is noticeably lowered compared to the previous experiment (480°C) with $P_{H_2} = 0.3$ atm.

Knowing the pressure of hydrogen in the exit gas and its inlet flow rate we have calculated the amount of hydrogen consumed at various times (Fig. 3). At the end of the reduction the total amount of hydrogen consumed corresponds to about 3.2 mol H_2 per mol W which shows, considering the margin of error of the measurements, that WO_3 is completely reduced into W at 600°C by hydrogen at 1 atm. The steps of reduction of WO_3 cannot be clearly distinguished in this experiment, but probably the maximum of hydrogen consumption at 600°C (minimum in Fig. 2) corresponds to the maximum rate of reduction of WO_3 into WO_2. The first step corresponding to the formation

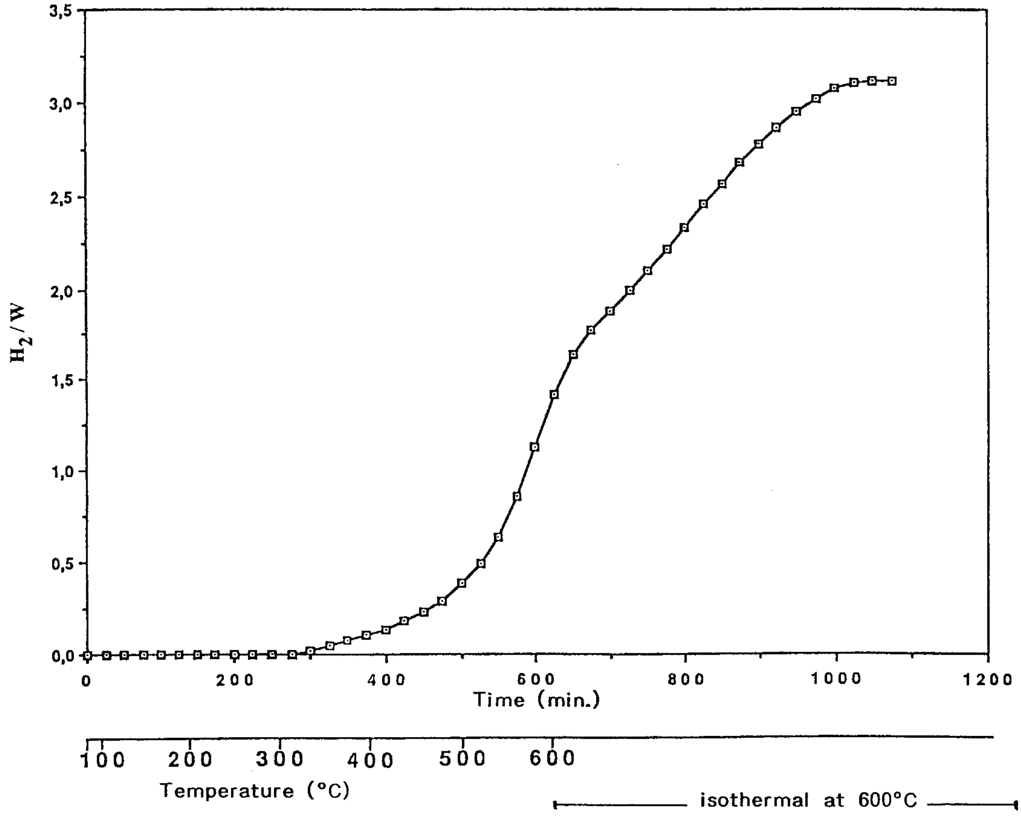

FIG. 3. Hydrogen consumption as a function of time during reduction of WO_3.

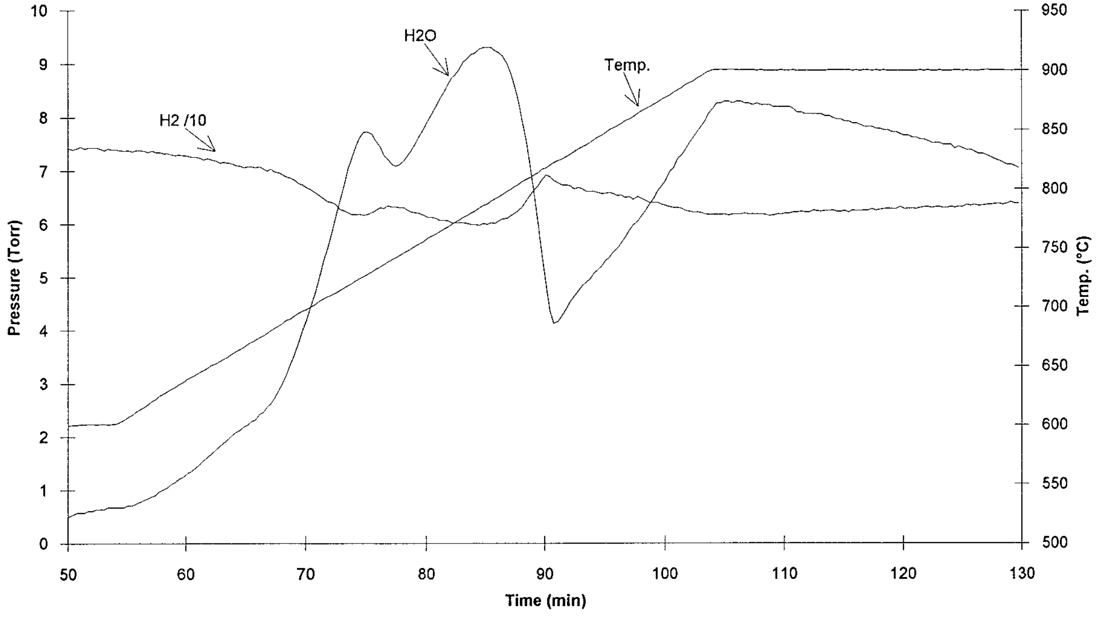

FIG. 4. Reduction of WO_3 in a mixture of 30% H_2 in Ar at atmospheric pressure heated at rate of 180°C h^{-1}. 74 mg.

TABLE 2

TPR Results under Various H_2 Pressures

		Temperatures (°C)			
			Maximum rate of formation		
P_{H_2} (Torr)	Heating rate (°C h^{-1})	Beginning of reduction	WO_{3-x}	WO_2	W
760	50	300–400	*	600	*
230	150	480	640	670	800
76	360	600	730	800	>900
1	180	700–750	*	>1000	*

* Not determined.

of a suboxide cannot be distinguished from the second one. The reduction of WO_2 into W metal probably mainly occurs during the almost constant H_2 consumption in the isothermal stage at 600°C. The heating rate was three times lower in this experiment than in the previous one. The separation of the steps $WO_3 \rightarrow WO_2$ and $WO_2 \rightarrow W$ is accordingly worse than that obtained with a lower H_2 pressure. In Fig. 3 the constant H_2 consumption starts at a ratio n_{H_2}/n_W of about 1.7, showing that, at 1 atm, the reduction of WO_2 into W metal starts much before the total reduction of WO_3 into WO_2. Taken overall, however, an increase of P_{H_2} from 0.3 to 1 atm has evidently increased the reduction rate.

1.3. Reduction by Hydrogen at a Pressure of 0.1 atm (Apparatus APR2)

WO_3 (Fluka, 76 mg) was reduced in a flowing mixture of 10% H_2 in argon ($P_{H_2} = 0.1$ atm) with a heating rate of 360°C h^{-1} from 600 to 900°C in apparatus APR2. The extent of reduction has been monitored using the height of the H_2O peak at mass 18 by mass spectroscopy. The results are given in Fig. 4 where we have plotted the hydrogen pressure and the temperature versus reduction time. Reduction starts only at around 600°C and clearly occurs in three steps. The position of the maxima are reported in Table 2. The third step starts at about 850°C but the position of the third peak maximum has not been determined since the experiment was stopped at 900°C.

It is evident that lowering the hydrogen pressure results in a considerable decrease in the rate of reduction of WO_3 into WO_{3-x} ($W_{18}O_{49}$ or $W_{20}O_{58}$), WO_2, or W metal, and consequently better separates the three steps of reduction. This effect of the hydrogen pressure indicates clearly that the rate limiting step of reduction is the surface reaction with hydrogen and not the diffusion rate of various species (probably W metal atoms) in the solid which should be independent of hydrogen pressure. Consequently, the com-

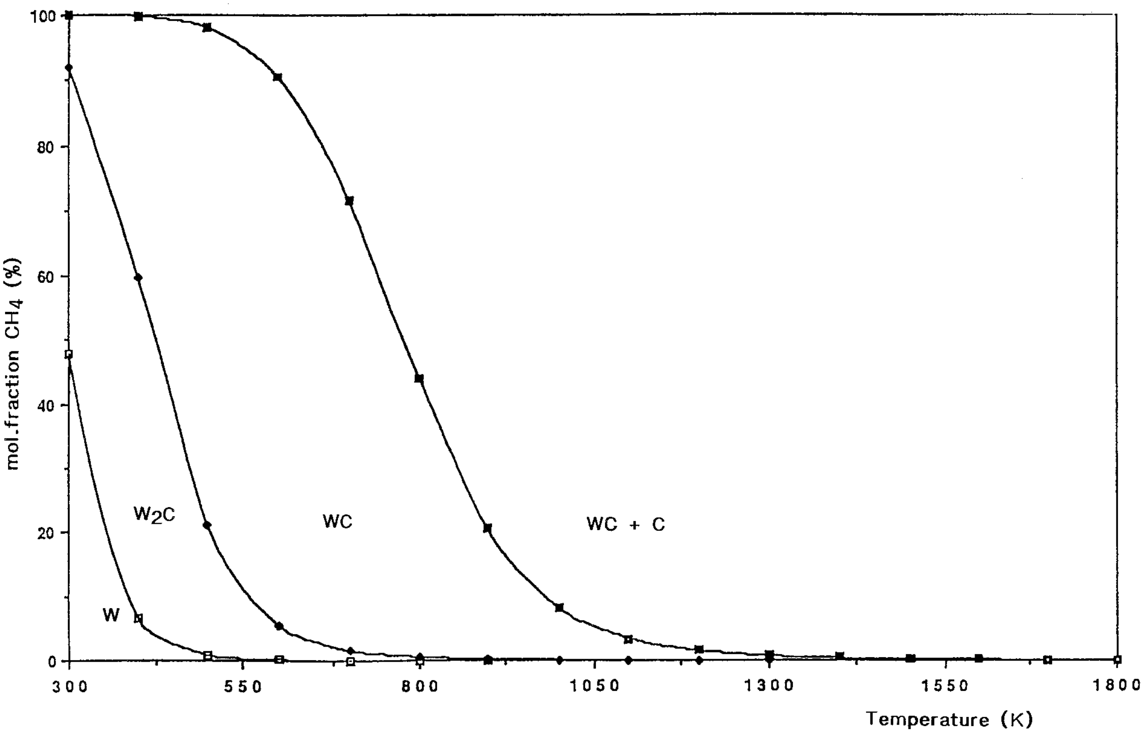

FIG. 5. Domains of existence for W, W_2C, WC pure, and with free carbon.

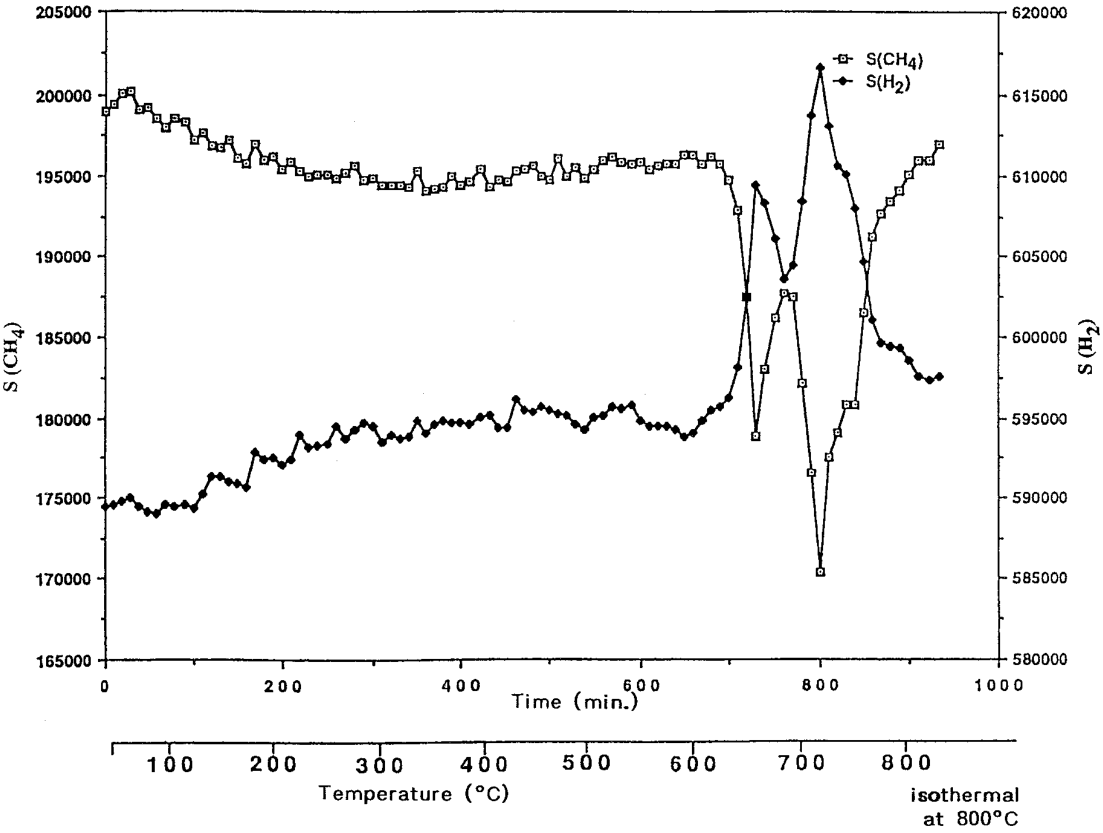

FIG. 6. Changes of the areas of H_2 and CH_4 chromatographic peaks versus time during temperature programmed carburization of W metal (50°C h^{-1}, 2.60 g W, 20% CH_4–H_2).

position of the solid is likely to be approximately uniform within the bulk of the solid whatever the extent of reduction.

2. Carburization of Tungsten Metal

2.1. Thermodynamics of the System $CH_4/W/C$

Three reactions are likely to occur during carburization of W:

$$2W + CH_4 = W_2C + 2H_2 \quad [1]$$

$$W_2C + CH_4 = 2WC + 2H_2 \quad [2]$$

$$CH_4 = C + 2H_2 \quad [3]$$

If a is the molar fraction of methane, then for each equilibrium the equilibrium constant is $K_i = (1 - a)^2/a$ if the total pressure is 1 atm. Using the thermodynamic data of Barin and Knacke (31) we have calculated the values of a corresponding to each equilibrium at various temperatures and at 1 atm total atmospheric pressure. The results are reported in Fig. 5 where we can see the domains of existence for W, W_2C, WC free of carbon or contaminated with carbon. Clearly, for the preparation of carbides free of carbon, it is better to use a carburizing mixture with a low molar fraction of methane. On the other hand, for very low CH_4 contents, the domains of existence of tungsten carbides are shifted toward higher temperatures and carburizing at too high a temperature could lead to solids with very low surface areas. Consequently we have decided to start this study of the carburization of W using a mixture containing 20% CH_4 in hydrogen with the same composition as the one often used by Boudart and co-workers (12–14, 32).

2.2. Carburization of Reduced WO_3 at 1 atm (Apparatus APR1)

2.2.1 Carburization with the mixture 20% CH_4–H_2: WCR1. The carburization of WO_3 (Fluka) reduced in hydrogen into W metal as described in the Experimental section was performed by temperature programmed reaction (13) at atmospheric pressure in a flow (10.2 liter h^{-1}) of the mixture 20% CH_4–H_2 increasing the temperature up to 800°C (50°C h^{-1}) where the sample was kept for 10 h. This sample was passivated according to the procedure

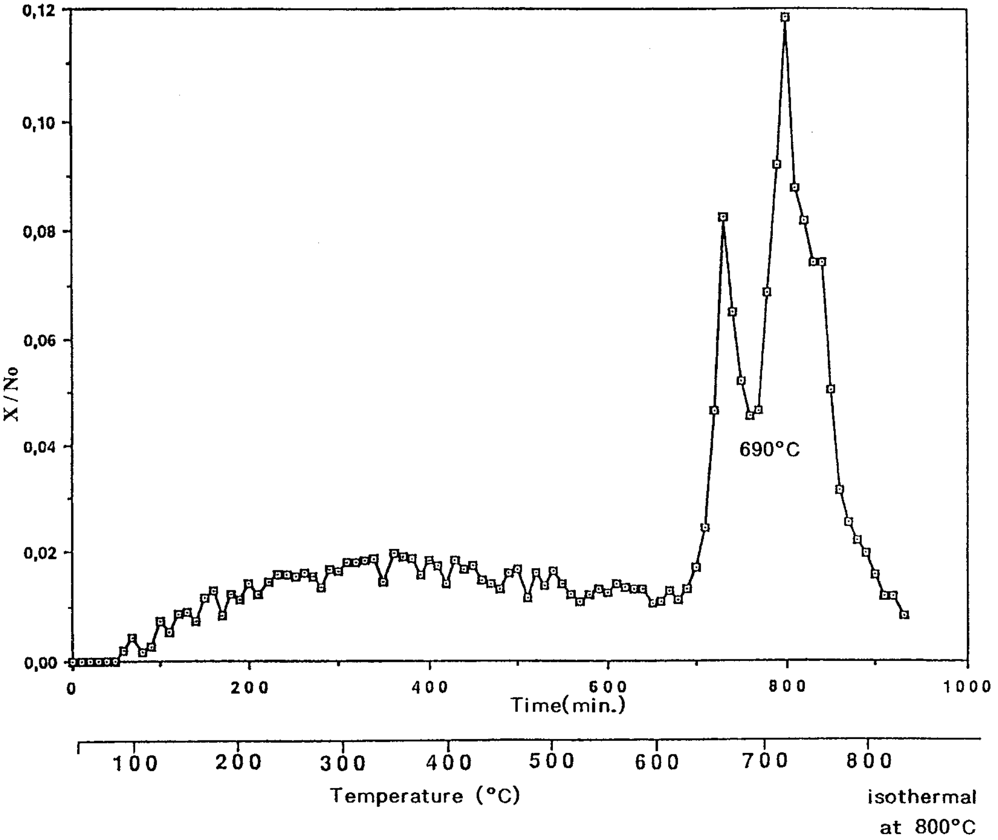

FIG. 7. Fraction of CH_4 consumed (X/N_0) as a function of time during temperature programmed carburization of W metal in 20% CH_4–H_2.

reported in the Experimental section. This solid will be called WCR1.

In Fig. 6, the areas of the chromatographic peaks (in arbitrary units) of CH_4 and of H_2, which are proportional to their partial pressures, are plotted versus time of reaction and temperature. At temperatures lower than 600°C a slight decrease in the methane partial pressure associated with a corresponding increase in the hydrogen partial pressure is observed. Then the composition of the mixture stabilizes at approximately 250°C. Methane consumption starts at about 600°C and exhibits two peaks respectively centered at 660 and 720°C. At 800°C the percentage of methane in the mixture reaches a value close to that observed between 250 and 600°C, but seemingly slightly lower.

When methane is consumed the hydrogen partial pressure increases, first, because of the lowering of methane partial pressure and second, because of hydrogen production during carbon consumption. To quantify the methane consumption, it is necessary to establish the relationship between the number of CH_4 molecules and the CH_4 pressure (proportional to the CH_4 signal in chromatography). In a very simple reasoning (see Appendix I) we have calculated the ratio X/N_0 of the molar flow rate of methane consumed at a given state of reaction to the initial one (here corresponding to 20% CH_4), as a function of the areas of CH_4 peaks and of a, the initial ratio of the molar fractions of hydrogen and of methane (here $a = 4$).

$$\frac{X}{N_0} = \frac{(a+1)[S(\mathrm{CH_4})_0 - S(\mathrm{CH_4})]}{(a+1)[S(\mathrm{CH_4})_0] + S(\mathrm{CH_4})}$$

$S(CH_4)$ is the area of CH_4 peak at a given time and $S(CH_4)_0$ is the initial area of the CH_4 peak. By integrating the curve (using the trapezium method), X/N_0 versus time (Fig. 7), we obtain the amount of CH_4 consumed as a function of time of carburization (Fig. 8).

The curve in Fig. 7 shows three regimes, the first starting at about 76°C, the second at 630°C (corresponding to the first peak in Fig. 6), and the third at 690°C. The two waves at 630 and 690°C correspond to real CH_4 consumption. However, the first feature probably does not correspond to CH_4 consumption; it is very likely to be a simple artefact due to different changes of hydrogen and of methane flow rates as a result of changes in the pressure drop due to the presence of the catalyst when the temperature increases. This results in changes of the mixture composition

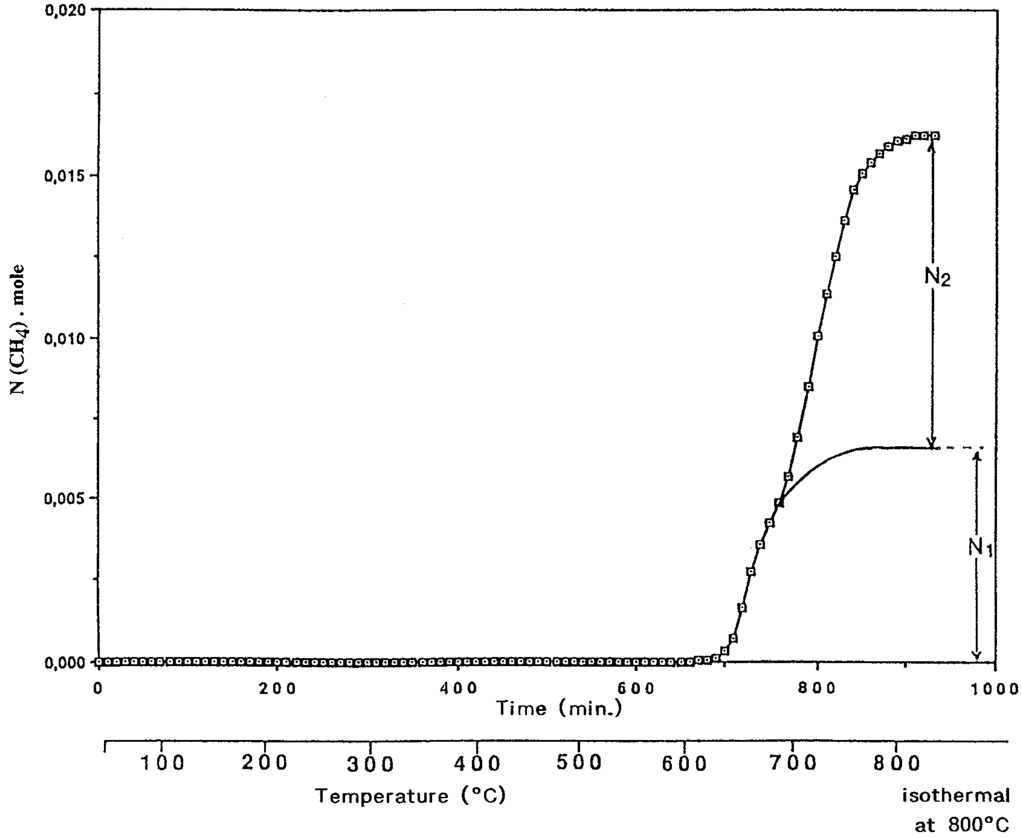

FIG. 8. Number of CH_4 moles consumed versus time during temperature programmed carburization of W metal in 20% CH_4–H_2.

and in a drift of the baseline. To support this view, let us mention that if this first regime is considered as resulting from CH_4 consumption the total amount of CH_4 used in this carburization would be 3.41×10^{-2} mol CH_4. Comparison of this value to the amount of W in the sample leads to a ratio CH_4/W of the number of molecules of CH_4 leading to C deposit to that of atoms of W of 2.2. Chemical analysis gives a ratio C/W in the final sample of 1.2. Hence the integrated curve of Fig. 8 has been obtained by considering that CH_4 consumption starts only at 630°C. In such a case the final value of the ratio CH_4/W is 1.22, which is in good agreement with chemical analysis. Therefore, our methodology enables us to calculate the number of CH_4 moles used for the carburization of W and for carbon deposit resulting from CH_4 decomposition.

Carburization has been shown to occur in two very distinct steps, one starting at about 630°C and the other at 690–700°C. We have tried to estimate the number of moles of CH_4 (N_1 and N_2) used in each of these two steps, taking into account the fact that at the minimum (at 690°C) between the two peaks of the curve X/N_0 vs time (Fig. 7) the second step of carburization has already started while the first is not yet finished due to its rate decreasing because of the exhausting of the W. For the first step, $N_1 = 7.1 \times 10^{-3}$ mol C and $N_1/W = 0.5$, and for the second step, $N_2 = 1.01 \times 10^{-2}$ mol C and $N_2/W = 0.72$. Hence we can conclude that in the first step of carburization one obtains essentially W_2C, whereas WC is noticeably formed only at temperatures higher than 690°C. The C/W ratio of 1.2 indicates that some carbon deposit at the carbide surface occurs during the carburization of W at 800°C. The surface area of the final solid after passivation, measured by N_2 physisorption, is 8.6 m^2 g^{-1}. The X-ray diffraction pattern of this carbide WCR1 exhibits the main lines characteristic of the simple hexagonal structure of WC.

The W 4*f*, C 1*s*, and O 1*s* XPS spectra of the passivated product are reported in Fig. 9. The W 4*f* signal exhibits the doublet W $4f_{7/2,5/2}$ at binding energies of 32.2 eV (±0.2 eV) for W $4f_{7/2}$ and at 34.2 (±0.2 eV) for W $4f_{5/2}$ characteristic of tungsten carbide (11, 32). The left side of the peak indicates the presence of some oxide (W^{6+}) at about 38 eV for W $4f_{5/2}$.

The decomposition of the photopeak C 1*s* using a FWHM of 1.7 eV typical of photopeaks of C 1*s* level (34) shows the participation of three components. The first at lower binding energy (283.3 eV) is specific for carbon in

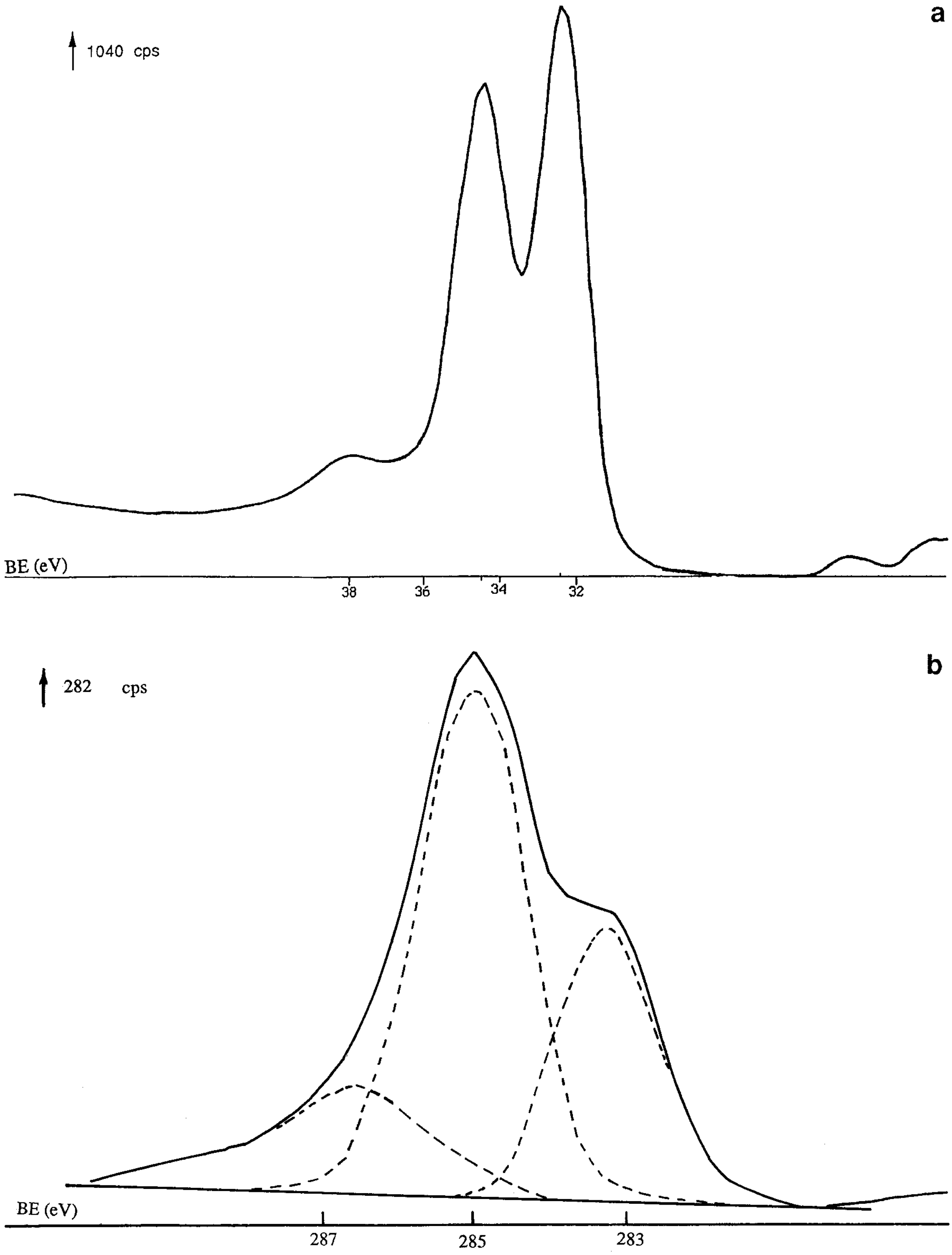

FIG. 9. XPS analysis of WC (WCR1) prepared by temperature programmed carburization of W metal up to 800°C in 20% CH_4–H_2. (a) W 4*f* photopeak; (b) C 1*s* photopeak; (c) O 1*s* photopeak.

a transition metal carbide (35). The highest peak at 285 eV is assigned to polymeric or free carbon and is a result partly of oil contamination in the spectrophotometer but mainly of carbon deposit arising from CH_4 decomposition. The third component is at higher binding energy (286.6 eV). Binding energies near this value (285.9 (35), 286.4 (34), and 286.7 (36)) have been reported in the literature for carbon atoms linked to oxygen atoms by single bonding in poly-ether-ether-ketones. Hence this third type of carbon can be attributed to surface carbon atoms bound to

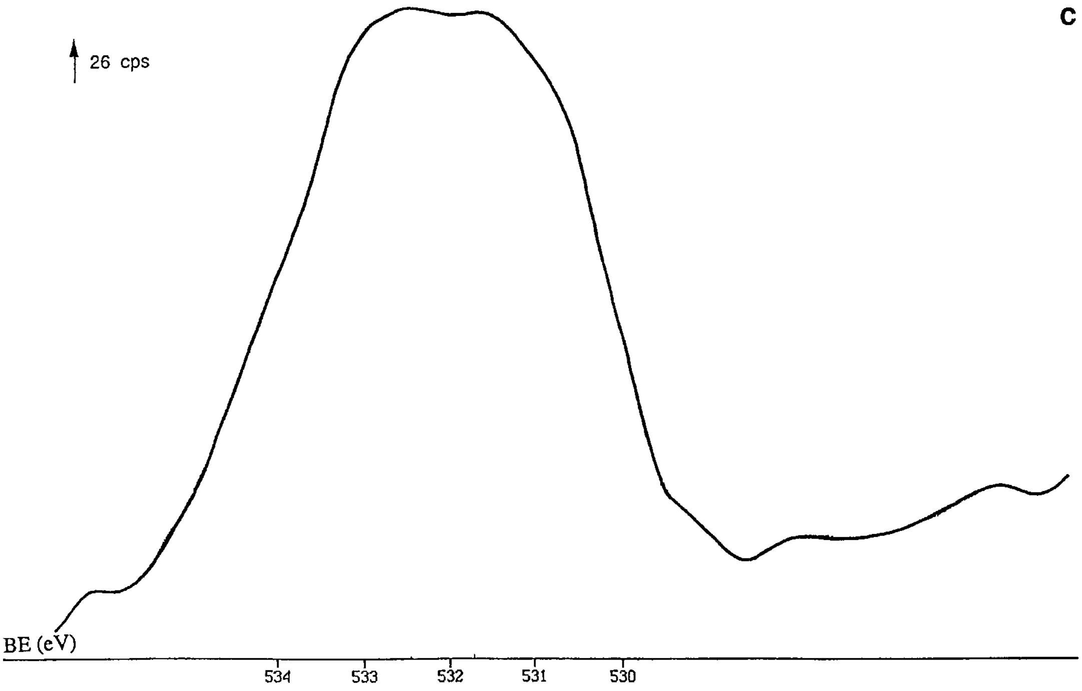

FIG. 9—*Continued*

oxygen of passivation. This last assignment is supported by the shape of the O 1*s* signal which is very wide (half width about 4 eV) and is composed of at least two components: there is one at 531.6 eV corresponding to transition metal oxides (37), while the other, centered at about 533 eV, could be attributed to oxygen in water (533 eV (38)) or hydroxyl groups (532.6 eV (39)) or to oxygen singly linked to carbon 533.8 eV (33) or 534.0 eV (34).

XPS results clearly show the formation of tungsten carbide. However, after carburization at 800°C, the surface of WC is covered with polymeric carbon and part of the carbide surface has been oxidized during passivation. This excess carbon and oxygen will have to be removed before catalytic reactions in order to characterize clean carbide surfaces.

The composition of the surface layers analyzed by XPS (about 5 nm in depth) is reported in Table 3. The C/W and O/W ratios determined by XPS analysis are definitely higher than those measured by chemical analysis. This shows that most of the "free" carbon and oxide phases are localized at the surface of the carbide.

2.2.2. Carburization of reduced WO_3 with the mixture 10% CH_4–H_2: WCR2. The thermodynamics of the WC/CH_4/C system predict an increase in the equilibrium temperatures for reactions [1–3] when the CH_4 percentage decreases, at 1 atm total pressure (Fig. 5). This could result in a lowering of the amount of free carbon at the surface. In order to check this, we have carried out carburization of W metal in a CH_4–H_2 mixture containing 10% of methane. The characteristics of this preparation are reported in Table 4. This sample was cooled from 800°C to room temperature in pure hydrogen. It is named WCR2. The variations of CH_4 partial pressure are reported in Fig. 10. CH_4 consumption starts at 685°C (a temperature that is higher than when 20% CH_4–H_2 was used), steeply increases and approximately stabilizes from 740 to 780°C, and slightly increases again up to 800°C where temperature was kept constant. The integration of the curve X/N_0 versus time of reaction leads to the curves in Fig. 11 where the ratio of CH_4/W of the number of moles of CH_4 consumed to that of W in the sample is plotted versus time and temperature. The value of CH_4/W corresponding to the end of the plateau of P_{CH_4} (780–785°C) is 0.5, which indicates that, at this stage, W_2C is likely to be formed; at the end of carburization at 800°C the ratio CH_4/W is 0.94. Chemical analysis gives the formula $WC_{0.91}O_{0.15}$ for this carbide WCR2, which is in good agreement with the previous result.

The X-ray diffraction pattern is characteristic of WC. The specific surface area (8 m^2 g^{-1}) is on the same order of magnitude as that of WCR1. The comparison of these results with those of the previous carburization in the mixture 20% CH_4–H_2 shows that, when the percentage of CH_4 is only 10%, CH_4 consumption starts at higher temperature (685°C instead of 630°C). Therefore a decrease in the CH_4 pressure results in a noticeable decrease in the carburiza-

TABLE 3

Bulk and Surface (XPS) Compositions and Specific Surface Areas of Bulk Tungsten Carbides

Catalysts	Temperature of carburization (°C)	Composition		XPS Characterization		Specific surface areas (m^2 g^{-1})
		From elemental analysis	From XPS	W_c/W_t	C_c/C_t	
WCR1	800	$WC_{1.22}O_{0.02}$	$WC_{3.4}O_{0.23}$	0.86		8.6
WCR2	800	$WC_{0.90}O_{0.15}$	$WC_{1.44}O_{0.83}$	0.64	0.55	8.0
WC1	900	$WC_{0.90}O_{0.2}$	$WC_{1.2}O_{0.80}$	0.69	0.62	10.2
WC2	600	$WC_{0.43}O_{0.66}$	$WC_{1.1}O_{1.3}$	0.52	0.56	11.6
WC3	630	$WC_{0.44}O_{0.74}$	$WC_{1.3}O_{1.5}$	0.50	0.56	21.0
WC4	660	$WC_{0.52}O_{0.50}$	$WC_{0.74}O_{1.0}$	0.68	0.65	not det.
WCR3	700	$WC_{0.86}O_{0.34}$	$WC_{1.30}O_{1.13}$	0.57	0.50	5.2
WC5	730	$WC_{0.90}O_{0.41}$	$WC_{2.7}O_{0.6}$	0.62	0.36	6.9
WCR4	900	$WC_{2.23}O_{0.01}$	$WC_{11}O_{0.3}$	0.87	—	11.4
WC6	900	$WC_{2.58}O_{0.01}$	$WC_{12.5}O_{0.4}$	0.88	—	15.0

tion rate. Here again, carburization seems to occur in two steps which would correspond to the formation of W_2C then of WC, but these two steps are not as well separated as with 20% CH_4–H_2. Both chemical (Table 3) and chromatographic analyses seem to indicate that a duration of 5 h in the isothermal stage at 800°C is not quite enough to carburize completely 4.3 g of WO_3 with the flow rates used here.

XPS analysis (Fig. 12) shows that tungsten (Fig. 12a) is in its carbidic form (W $4f_{7/2}$ at a BE = 32.8 eV) associated with a minor oxidic form (W $4f_{5/2}$ at a BE = 38.1 eV) that arises probably from passivation. This oxidic form is in a slightly higher proportion than in the previous sample carburized in 20% CH_4/H_2 which contained more free carbon at its surface. The C 1*s* photopeak (Fig. 12b) indicates that carbidic carbon (BE = 283.3 eV) is more abundant than the free carbon (BE = 285 eV) which is in contrast to what was obtained for WCR1. The maximum of O 1*s* is at 531.3 eV characteristic of oxygen associated with tungsten in oxide form. The broadening at higher binding energies probably originates from oxygen adsorbed on free carbon. The surface composition of WCR2 is reported in Table 3.

It is clearly seen that using a lower CH_4 pressure leads to less pollution of the carbide surface with free carbon. However, despite a possible global carbon deficit of the carbide, excess free carbon is deposited at the surface but at a much lower extent than when 20% CH_4–H_2 is used. Moreover, this carbon deficit does not seem to manifest itself at the surface ($C_c/W_c = 1.2$). As a consequence of lower carbon deposit, oxygen enters to a higher extent during the passivation step and the tungsten carbide surface is more oxidized ($W_c/W_t = 0.64$ and $O/W = 0.83$ against 0.86 and 0.2 for WCR1).

As a partial conclusion, the carburization of W metal with a mixture CH_4–H_2 is faster when the CH_4 pressure is increased and allows one to distinguish better between the two steps of carburization, but it increases the carbon deposit at the carbide surface.

2.3. *Carburization of Reduced WO_3 at 5 Torr* (*Apparatus LPR*)

WO_3 (Fluka, 76 mg) was reduced under 100 Torr of hydrogen at 1000°C for 1 h. The surface area of W metal measured by the Kaganer method (26) is very low: 0.1 m^2 g^{-1}. Then it was submitted to a flow of 6% CH_4–D_2 mixture, at a total pressure of 5 Torr with a heating rate of 360°C h^{-1} from 25 to 1000°C. Changes in the methane partial pressure and the temperature versus time are reported in Fig. 13. The amount of CH_4 does not change until 750°C, and then one can observe a sudden decrease in CH_4 at partial pressure between 750 and 815°C. This decrease is not accompanied with increases in the heights of peaks at mass 17 to 20, hence there is no CH_4–D_2 exchange. In contrast, a corresponding increase in the heights of peaks at mass 2 and 3 indicates that methane is decomposed into carbon and hydrogen adsorbed at the surface allowing dihydrogen desorption and exchange between deuterium and H adsorbed, and, probably, the beginning of W carburization.

The complete absence of deuterated methane clearly indicates that each molecule of CH_4 which becomes adsorbed on W at 1000°C does not desorb but remains on the solid and is decomposed. It should be noted that a tremendous decrease in CH_4 pressure from 76 Torr (0.1 atm) to 0.25 Torr only results in a modest increase in the temperature of the beginning of CH_4 consumption from 685 to 750–815°C.

TABLE 4

Experimental Conditions of Preparation of Bulk Tungsten Carbides at Atmospheric Pressure

		Preparation				Posttreatment in H_2				Passivation		
Catalyst	Precursor weight (g)	F^a (liter h^{-1})	T (°C)	G^b (°C h^{-1})	Duration (h)	F (liter h^{-1})	T (°C)	Duration (h)	Cooling to RT	F (liter h^{-1})	% O_2	Duration (h)
WCR1	WO_3	TN^c = 9.95	550	50	10		No		$CH_4 + H_2$	11.0	1.4	15
	3.27	TR^d = 8.0	600	50	10							
		TC^e = 10.2	800	50	10							
WCR2	WO_3	TN = 3.6	500	60	14		No		H_2	3.5	2.0	15
	4.35	TR = 3.6	600	60	12							
		TC = 3.1	800	60	5							
WC1	Ammonium	TN = 10.0	550	50	10							
	metatungstate	TC = 10.4	900	50	10	8.3	800	5	H_2	10	1.0	15
	3.51											
WC2	WO_3	TN = 9.7	550	50	10		No		$CH_4 + H_2$	8.5	0.5	15
	3.14	TC = 10.0	600	50	33							
WC3	WO_3	TN = 10.1	550	50	10		No		$CH_4 + H_2$	10.3	0.6	15
	3.11	TC = 10.3	630	50	28							
WC4	WO_3	TN = 6.0	550	60	5		No		H_2	3.0	2.0	15
	1.02	TC = 6.1	660	60	4							
WCR3	WO_3	TN = 2.5	500	30	10		No		$CH_4 + H_2$	3.0	2.0	15
	5.20	TC = 2.7	600	30	10							
		TC = 3.4	700	30	10							
WC5	WO_3	TN = 10.2	550	50	10		No		$CH_4 + H_2$	8.9	1.3	15
	3.37	TC = 10.9	730	50	10							
WCR4	WO_3	TN = 10.1	550	50	10		No		$CH_4 + H_2$	10.1	1.6	15
	3.53	TC = 8.2	600	50	11							
		TC = 11.0	900	50^f	15							
WC6	WO_3	TN = 10.4	550	50	10		No		$CH_4 + H_2$	10.0	0.6	6
	3.72	TC = 10.0	900	50^f	6							

[a] Flow rate (liter h^{-1}).

[b] Gradient of temperature (°C h^{-1}).

[c] Treatment in N_2.

[d] Treatment of reduction.

[e] Treatment of carburization.

[f] 50°C h^{-1} from RT to 450°C, then by steps of about 10 h every 30°C.

The integration of the amount of CH_4 decomposed corresponds to a ratio C/W of 0.99.

3. Carburization of Unreduced WO_3

3.1. Carburization at 1 atm (20% CH_4–H_2): WC1 (Apparatus APR1)

In their papers on tungsten carbide preparation, Boudart and co-workers (12–14) state that they have directly carburized WO_3 without previous reduction. Hence we have studied the carburization of samples of a few grams of WO_3. Here the precursor WO_3 (1.42×10^{-2} mol) was prepared by metatungstate decomposition. The maximum temperature of carburization was 900°C, a temperature at which the sample was left for 10 h.

During this experiment the chromatographic analyses indicated, besides CH_4 and H_2 consumption, the formation of H_2O, CO, and CO_2. The composition of the gas flowing at the outlet of the reactor is reported in Fig. 14.

The curve of H_2O formation is very much like that obtained during TPR of WO_3 with the mixture 30% H_2–Ar, but it is shifted toward lower temperatures as expected with a hydrogen pressure of 0.8 atm instead of 0.3 atm. Starting at 550°C, CO production occurs, it is maximum at 740°C, and it continues until 900°C. It is accompanied

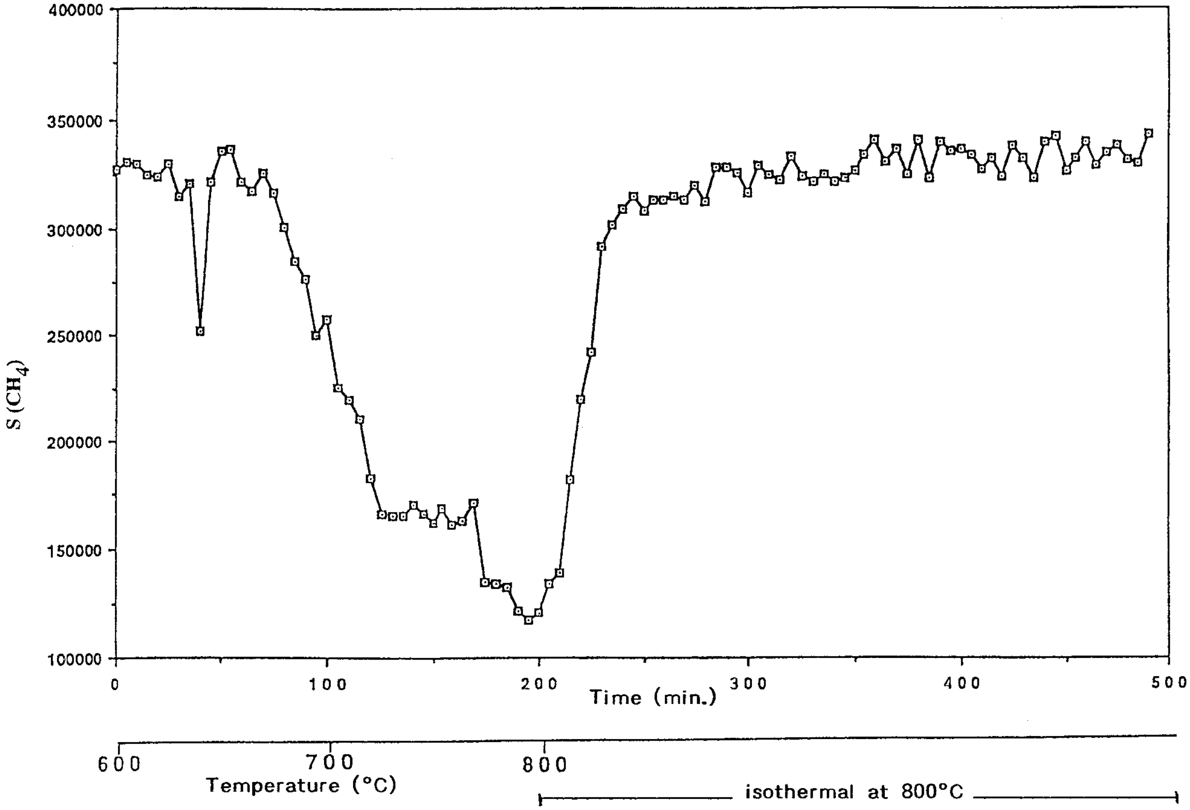

FIG. 10. Changes of the area of the CH_4 chromatographic peak versus time during temperature programmed carburization of W metal (60°C.h^{-1}, 4.35 g, 10% CH_4–H_2).

by CO_2 from 700°C. CO and CO_2 are produced during tungsten oxide reduction either directly in reactions such as

$$WO_3 + CH_4 = WO_2 + CO + 2H_2 \quad [4]$$

$$WO_2 + 2CH_4 = W + 2CO_2 + 4H_2 \quad [5]$$

$$WO_2 + CH_4 = W + CO_2 + 2H_2, \quad [6]$$

or in methane reforming by H_2O produced in the reduction of WO_3 with H_2:

$$CH_4 + H_2O = CO + 3H_2 \quad [7]$$

$$CH_4 + 2H_2O = CO_2 + 4H_2. \quad [8]$$

Reactions [7] and [8] are catalyzed by transition metals (40, 41) and they usually occur at temperatures between 600 and 800°C, as in this experiment. At this stage, we cannot identify the principal steps leading to CO and CO_2 production. However, in each of the reactions [4] to [8], the disappearance of one molecule of CH_4 is accompanied by the formation of three molecules (one of CO or CO_2 and two of H_2) in the gas phase. By the simple calculation reported in Appendix II we have calculated the ratios X/N_0 (already defined), and Y/N_0, Z/N_0, N_{H_2O}/N_0 using the areas of the various product peaks. X, Y, and Z are the number of CH_4 moles consumed for carburization and carbon deposit (X), and for CO and CO_2 formation (Y and Z) per unit of time, and N_{H_2O} is the number of molecules of water formed per unit of time.

Then one can plot the curves of X/N_0 and $(Y + 2Z + N_{H_2O})/N_0$ as a function of time which represent, respectively, the relative amounts of carbon consumed (for carburization and carbon deposit) and of oxygen eliminated in WO_3 reduction. Their integrations lead to the curves in Figs. 15 and 16. The total amount of oxygen in H_2O, CO, and CO_2 formed (Fig. 16) corresponds to an O/W ratio of 3.14 which shows that all WO_3 has been reduced into W^0 in the reaction. The amount of oxygen consumed during the first peak of reduction (max: 630°C) corresponds to a ratio O/W close to 1.4. Hence, at that temperature WO_3 is reduced into WO_2 but also some W metal is already formed.

Coming back to Fig. 14, a decrease in CH_4 pressure is noticeable from 600°C, and the pressure then goes through a mild minimum around 650°C, increases slightly before

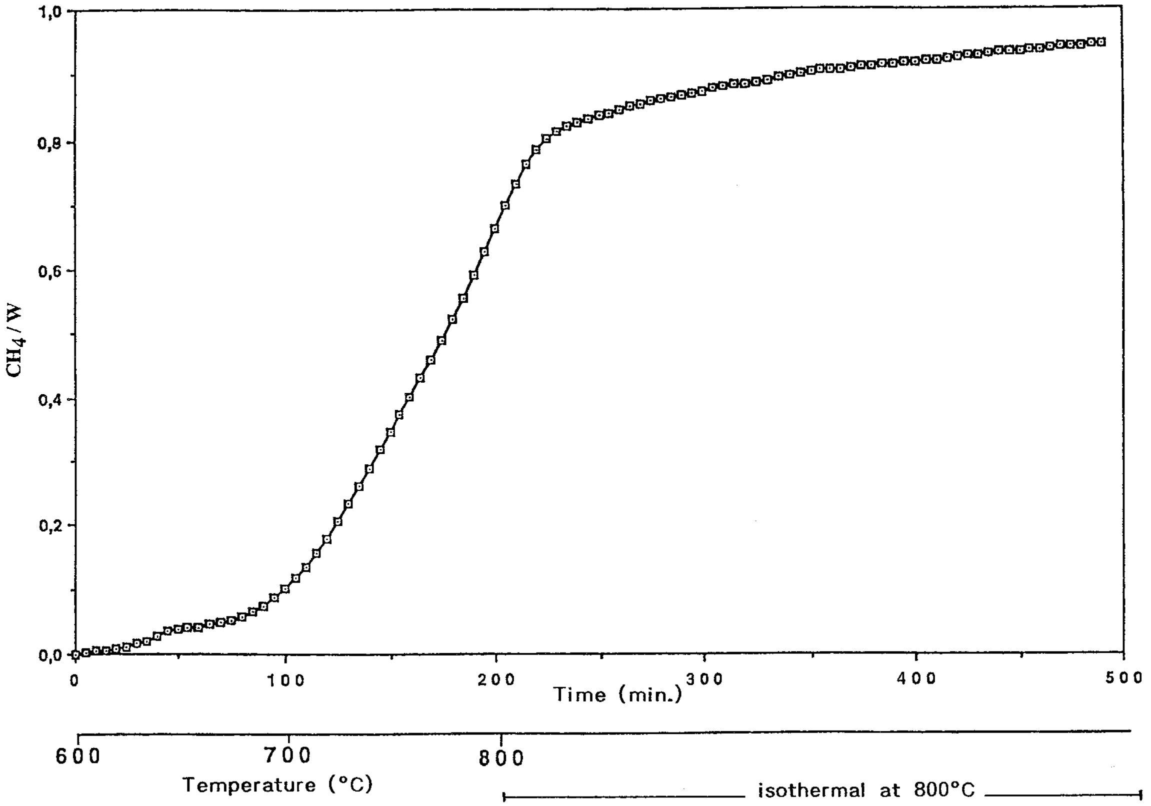

FIG. 11. Ratio of the number of CH_4 moles consumed to that of W metal versus time during the temperature programmed carburization of W metal in a 10% CH_4–H_2 mixture.

decreasing again at 720°C, and goes through two minima at 750 and 785°C. From Fig. 15, one can estimate the ratios C/W corresponding to these three peaks (Table 5).

In this case the carbon consumption in the first step of carburization (600–720°C) is much lower than that corresponding to the first step of carburization of W metal into W_2C (C/W = 0.5). Here, only around 50% of tungsten would have led to W_2C. From Fig. 16, the amount of oxygen consumed up to 720°C, which corresponds to the end of the first peak of carburization, is 2.8×10^{-2} mol O, an amount which allows the complete reduction of WO_3 into WO_2 (1.42×10^{-2} mol O) and of 48.5% of WO_2 into W metal. These figures seem to indicate that only W metal can be carburized by CH_4. The explanation for the second and the third peaks of CH_4 consumption is not easy. The second peak could correspond to the completion of W_2C formation together with the beginning of WC formation and of free carbon deposit. The third peak could be due to the end of WC formation accompanied by free carbon deposit.

The total amount of C consumed in this experiment (C/W = 1.51) is higher than that in the preparation of WCR1. This shows that at 900°C carbon deposit is more important than at 800°C.

After a treatment in flowing hydrogen for 5 h at 800°C and passivation, chemical analysis indicates a composition corresponding to $WC_{0.9}O_{0.2}$ which shows that the hydrogen treatment removes most of the free carbon. X-ray diffraction shows that the solid obtained in this preparation is the hexagonal WC.

W 4*f*, C 1*s*, and O 1*s* XP spectra are very similar to those obtained for WCR2 (Fig. 12). Table 3 shows that the resulting solid is tungsten carbide and that the amount of free carbon is low (C/W = 1.2), but also that part of tungsten carbide was more oxidized during passivation (W_c/W_t = 0.69) than WCR1 which had not been treated in a flow of pure hydrogen after carburization.

The temperature programmed carburization at 1 atm of WO_3 (Fluka) in a flow of 20% CH_4–H_2 was also studied *in situ* by X-ray diffraction. In the X-ray diffractometer, the sample was submitted to drying (RT to 550°C) and carburizing treatments similar to those of the previous sample WC1 up to 800°C where it was left for 5 h. An X-ray diffraction pattern was registered every 100°C up to 500°C, then every 50°C during the temperature programming, and after every hour during the isothermal treatment.

The various X-ray diffraction patterns are reported in

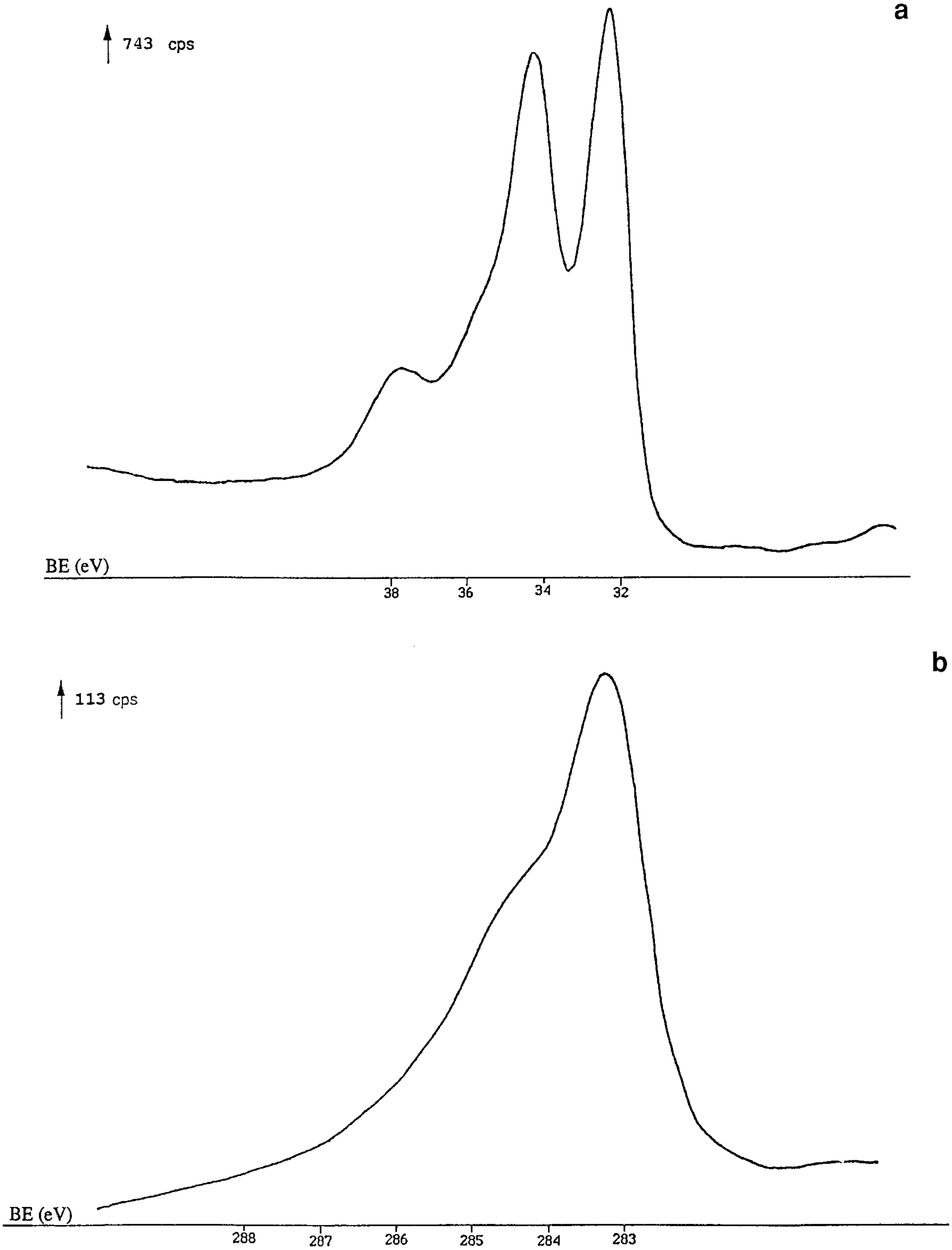

FIG. 12. XPS analysis of WC (WCR2) prepared by temperature programmed carburization of W metal up to 800°C in 10% CH_4–H_2. (a) W 4*f* photopeak; (b) C 1*s* photopeak; (c) O 1*s* photopeak.

Fig. 17. During the N_2 drying treatment no change occurs; only WO_3 is present. During the carburizing treatment, noticeable modifications begin to be observed at 500°C where a small amount of some new phases were formed which were difficult to identify with certainty but which could be hydrogen bronzes or/and tungsten suboxides. At 550°C, $W_{20}O_{58}$ and bulk W_3O (or W_3C) can be identified. However, no WO_2 has been detected by XRD. At 600°C the pattern is completely modified and indicates the presence of a single phase which is either W_3O or W_3C (Fig.

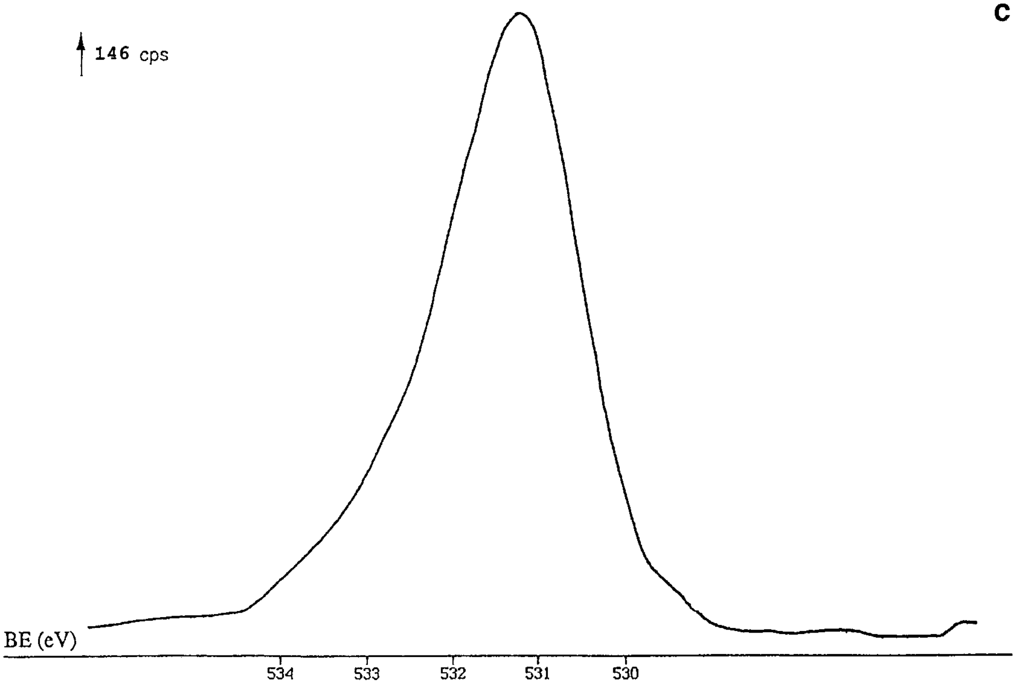

FIG. 12—*Continued*

18). At 650°C a small proportion of carbide which could correspond to $W_6C_{2.54}$ or to W_2C is formed. Then, at 700 and 750°C, only W_2C is observed and finally at 800°C WC is progressively formed at the expense of W_2C which disappears almost completely after 2 h of isothermal treatment at 800°C.

This XRD study is in good agreement with the previous experiments, since it indicates a progressive reduction of WO_3 starting at about 500°C. No W metal has been detected by X-ray diffraction, but the formation of W_2C when W_3O (or W_3C) disappears probably indicates that with a CH_4 pressure of 0.2 atm, W metal is almost immediately transformed into W carbide. The progressive carburization of W, first into W_2C and then into WC, has been evidenced here.

3.2. Carburization at Low Pressures (Mixtures of 20% CH_4–H_2 from 0.3 atm to 0.5 Torr)

3.2.1. Carburization at mixture pressures of 0.3 atm and 0.1 atm (apparatus APR2). The carburizing mixture was composed of 20% CH_4/H_2 (0.1 or 0.3 atm) diluted with argon.

The variations of the composition of the products flowing out of the reactor were rather similar to those observed with sample WC1 (Fig. 14) during the carburization at atmospheric pressure, but they are shifted toward higher temperatures (Table 6).

A low production of CO has been observed between 600 and 810°C at 0.3 atm and between 830 and 1000°C at 0.1 atm. The total amount of oxygen consumed corresponds to a ratio O/W close to 3, indicating that WO_3 has been completely reduced into W metal.

In the experiment performed at 0.3 atm, CH_4 consumption is important at temperatures between 760 and 840°C. It starts very slightly at lower temperatures (about 600°C) but carbon mass balance shows that CH_4 is mainly transformed into CO. The real CH_4 consumption for carburization starts only at 760°C; that is at a much higher temperature ($\Delta T = 160°C$) than during carburization at 1 atm. The difference is even much more important for the experiment at 0.1 atm since, there, CH_4 consumption begins at about 870°C, is roughly constant up to 970–980°C, sharply increases at 980°C, and finally decreases and becomes negligible. The first consumption of CH_4 up to 980°C corresponds only, or mainly, to CO production and the second sharp CH_4 peak is due to carburization which occurs when a large part of WO_3 has been reduced into W metal. Hence, at lower CH_4 pressure the relative position of the peak of carburization compared to that of the W formation is shifted toward higher temperatures. Such a behavior can easily be understood on the basis of two competitive phenomena occurring to W metal formed at the surface of the solid. The first is its carburization and the second is the diffusion of W atoms from the surface into the bulk of the sample. The diffusion of W metal is unaffected by CH_4 pressure and it was shown previously to be fast compared

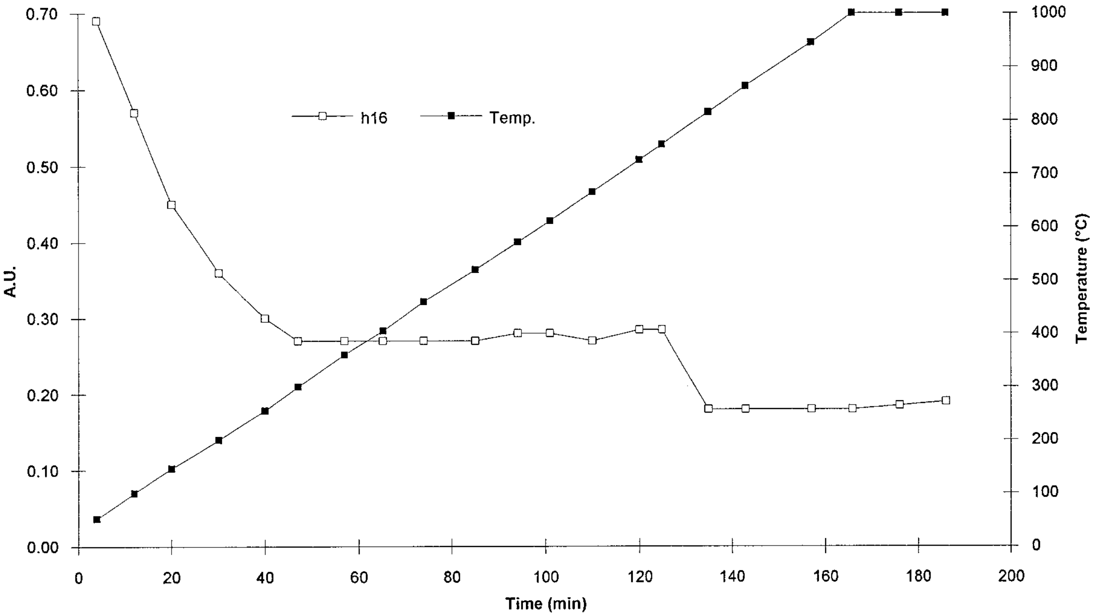

FIG. 13. Temperature programmed carburization of W metal at 5 Torr. Change of CH_4 pressure versus time (360°C h^{-1}, 76 g WO_3, 20% CH_4–D_2).

to the rate of reduction of W oxides by H_2. In contrast, the carburization of W metal is probably very much lowered by a decrease of CH_4 pressure. Hence, if the diffusion of W is much faster than its carburization one can understand that carburization of W occurs only when a large part of W oxide has been reduced into W.

The stoichiometry of the final product carburized at 0.1 atm has been determined by temperature programmed oxidation from the amounts of CO and CO_2 produced during TPO. It corresponds to the formula $WC_{1.1}$ which is very close to WC.

The total carbon consumption in the carburization at 0.3 atm corresponds to a ratio C/W close to 1.44. This indicates that the CH_4 pressure has a large importance for the amount of free carbon at the surface of the catalyst since the ratios C/W are 1.51, 1.44, and 1.1 for temperatures of carburization, respectively, of 900, 840, and 1000°C in CH_4–H_2 mixtures at pressures of 1, 0.3, and 0.1 atm.

3.2.2. Carburization at a total pressure of 5 Torr (apparatus LPR). The reactions that can take place during this experiment are numerous, thus there are the reduction of WO_3 by D_2 and by CH_4 (which will form CO and CO_2), the exchange of CH_4 with D_2 or with D_2O formed by the reduction of WO_3, and the consumption of methane for the carburization or for free carbon formation (decomposition of CH_4). Information on this last reaction of methane consumption is given by the height of the peak at $m/z = 12$ (h_{12}) independently of the exchange of CH_4. It has been observed (Fig. 19) that, within the margin of error, the total methane pressure is constant until the solid has been kept at 1200°C for 15 min, and then it decreases while carburization starts to take place.

CH_4 exchange is better followed by the height of the peak at $m/z = 15$ (h_{15}) than by h_{16}, since water decomposition participates at mass 16. One can observe (Fig. 20) that, up to about 1000°C, no methane exchange occurs, and then its importance continuously increases with temperature. It is interesting to notice that the temperature where CH_4 exchange starts to take place is the same as that where H_2 and HD appear in the gas phase (Fig. 21). Therefore, probably, CH_4 exchanges hydrogen atoms with D_2 and not with D_2O. Peaks at $m/z = 17$, 18, 19, and 20 start to increase at the same temperature, about 650°C, which corresponds to the beginning of the reduction of WO_3 by D_2; then they go through maxima (at the same temperature for $m/z = 17$, 18, and 20) and become negligible after about 30 min at 1000°C indicating that the reduction of WO_3 is complete. The simultaneous increase of peaks at mass 20 and 17 to 19 indicates that exchange between D_2O and some hydrogen-containing species occurs. However, since no CH_4 is exchanged before 1000°C, HDO is probably formed at lower temperatures by exchange of D_2O with some hydroxyl groups at the surface of WO_3 or with some water molecules of crystallization of WO_3. Let us notice that, at 1000°C, the height of peak 19 increases much more rapidly when the temperature increases than that of peak 20 (Fig. 22), probably in relation to CH_4 exchange which gives HDO. Moreover, the height of peak 17, which was very low, suddenly increases at that temperature, very probably and in the main because of

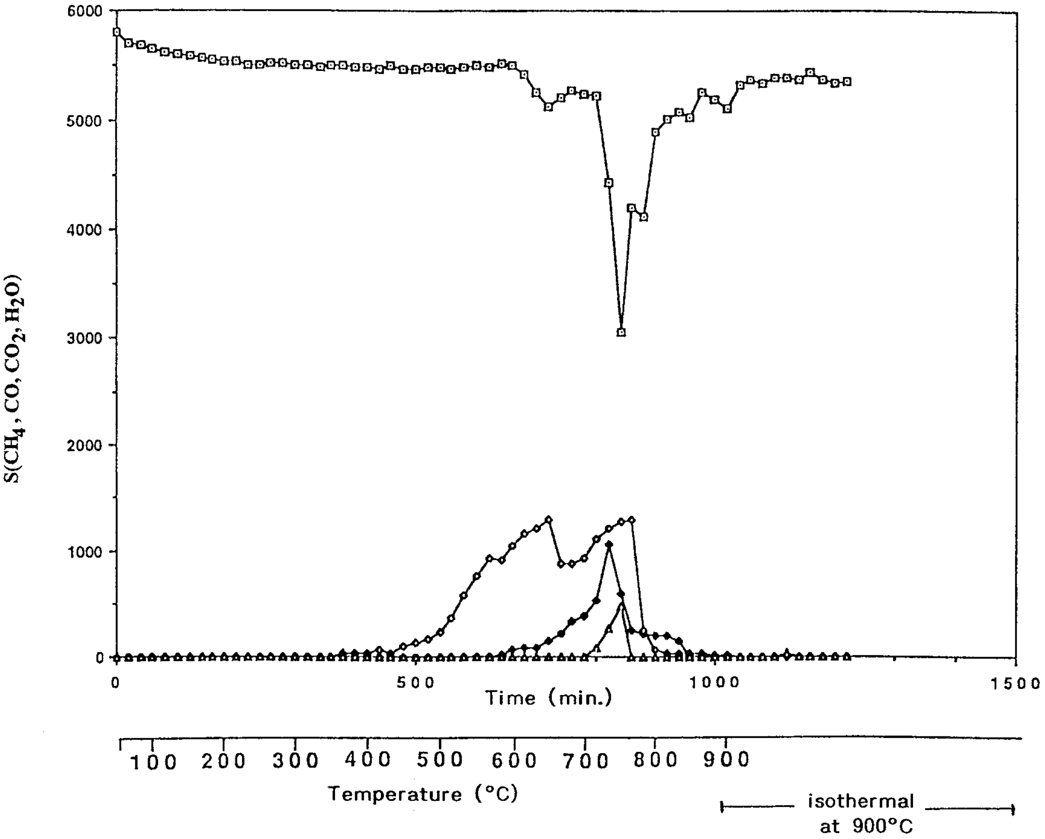

FIG. 14. Changes of the area of CH_4, H_2O, CO, and CO_2 chromatographic peaks (normalized, taking into account the relative molar response of the TCD) during the temperature programmed carburization of WO_3 (50°C h^{-1}, 3.51 g ammonium metatungstate, 20% CH_4–H_2). □ $S(CH_4)/36$; ◆ $S(CO)/42$; ◇ $S(H_2O)/33$; △ $(S(CO_2)/48) \times 30$.

the formation of CH_3D. An argument for the assignment of peak 17 mainly to CH_3D after 1000°C can be found when considering the ratio of the heights of peaks 17 and 19 (Table 7) (these heights have to be corrected for the residuals). This ratio is roughly constant until 1000°C and is approximately equal to 0.12 ± 0.02 which is characteristic of HDO fragmentation into HO^+. Then it noticeably increases with temperature because of CH_3D formation. In contrast, the ratio $h_{18}/(h_{20} + h_{19})$ is roughly constant whatever the temperature, which indicates that h_{18} mainly, if not only, originates from D_2O and HDO fragmentation.

CO and CO_2 were also observed at high temperature (approximately from 830 to 860°C).

The comparison of the curves in Fig. 19 (CH_4 consumption) and 22 (water production) indicates that carburization occurs only when the reduction of WO_3 is complete (end of water formation). This is very well explained by a very fast migration of W metal atoms into the bulk of the sample and, since at such a low CH_4 pressure of 1 Torr the rate of carburization is certainly very low, carburization cannot occur before complete WO_3 reduction into W metal which occurs after about 15 min at 1200°C (Fig. 22).

3.2.3. Carburization at a total pressure of 0.5 Torr (apparatus LPR). At such a low pressure, peaks 17 to 20, which indicate the formation of water, hence the occurrence of tungsten oxide reduction, start to increase at only about 800°C, the temperature where CO starts to appear. Hence at that pressure, water and carbon monoxide are simultaneously formed. No decrease in the height of peak 16 has been observed. Moreover, no formation of H_2 or of HD has been detected. Hence, no CH_4 exchange with D_2 takes place, indicating that no W metal is present at the surface of the solid. Consequently no carburization can occur. A further analysis has confirmed these conclusions, since only an amount of carbon corresponding to 0.5% of the W atoms present has been detected, which corresponds to surface carbon deposit.

4. Influence of the Maximum Temperature of Carburization

The maximum temperature of carburization was varied between 600 and 900°C. In each case, this temperature was maintained constant for several hours. The experimental

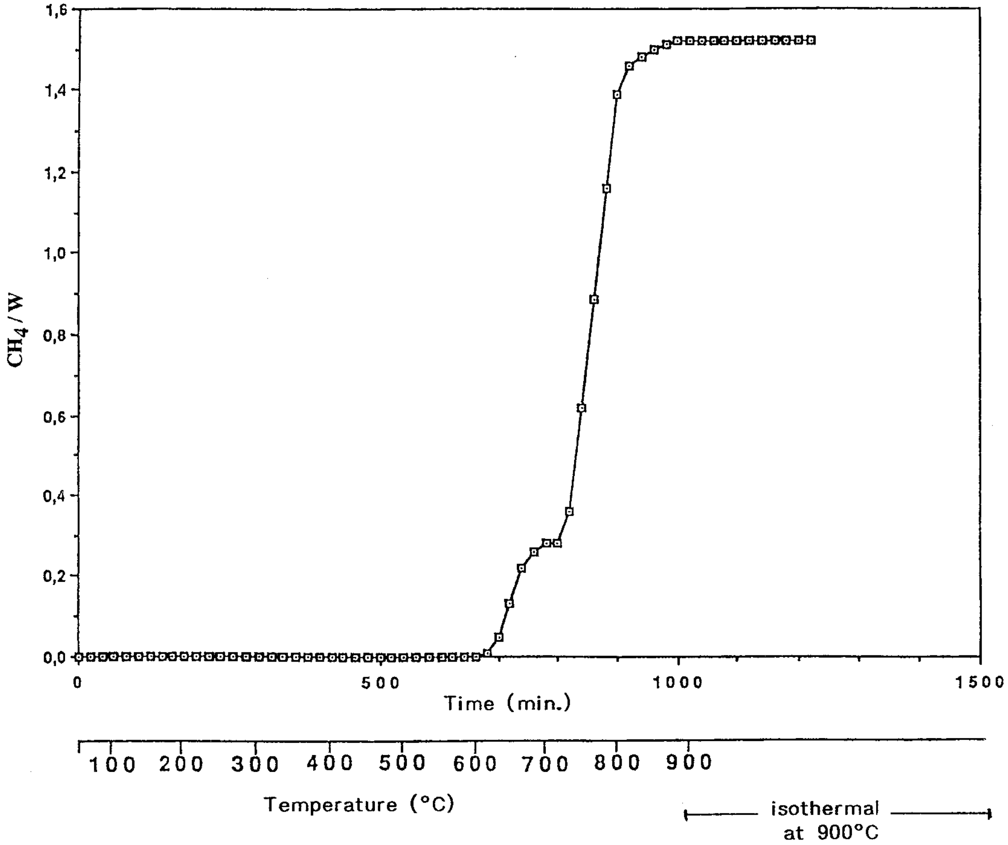

FIG. 15. Ratio of the number of CH_4 moles consumed to that of W versus time during the temperature programmed carburization of WO_3 in 20% CH_4–H_2.

conditions of preparation of the various samples are summarized in Table 4 and their compositions (elemental analysis and XPS) together with their physical and chemical characterizations are in Table 3.

At 600°C (sample WC2), the solid obtained is a mixture of W_2C, W metal, and probably W oxycarbide as seen by X-ray diffraction. Its overall formula is $WC_{0.43}O_{0.66}$. Hence 600°C is too low a temperature to obtain pure tungsten carbides. In contrast, a temperature of carburization of 630°C (WC3) or 660°C (WC4) leads to pure W_2C (checked by XRD). The amount of CH_4 consumed during the preparation of the sample WC3 corresponds to a ratio C/W of 0.52. Its overall composition after 1 year storage in air was $WC_{0.44}O_{1.1}$, which shows that it has been heavily oxidized. For these three compounds, XPS analysis (Table 3) indicates the presence of W carbide and oxide together with carbidic carbon and carbon of pollution. The proportions of carbidic C (C_c/C_t = 0.56 and 0.65) and of W oxides (W_o/W_t = 0.32 and 0.5) are high, indicating that, at these low temperatures, the amount of free carbon is low, and consequently it cannot play its protecting role during the passivation step, leading to significant surface oxidation of W_2C.

Carburization at 700 or 730°C (samples WCR3 and WC5) leads to mixtures of W_2C and WC (XRD and elemental analysis, Table 3) with a large predominance of the WC phase. After carburization at higher temperatures (800 to 900°C) the only phase detected by X-ray diffraction is WC.

It is interesting to note that, according to the selected temperature of carburization, it is possible to synthesize pure W_2C or WC.

Table 3 clearly shows that the higher the temperature of carburization the higher the proportion of free carbon and the lower the proportion of W oxide after passivation.

CONCLUSION

This study of the carburization of W metal and of WO_3 by CH_4–H_2 mixtures has clearly shown that it occurs in two distinct steps. W_2C is formed in the first step at about 650–700°C in a CH_4 pressure of 0.2 atm, while WC is formed in the second step. Hence it is possible to synthesize either W_2C or WC by adjusting the conditions of carburization (mainly the temperature). It has also been shown that the rate of reduction of WO_3 together with that of

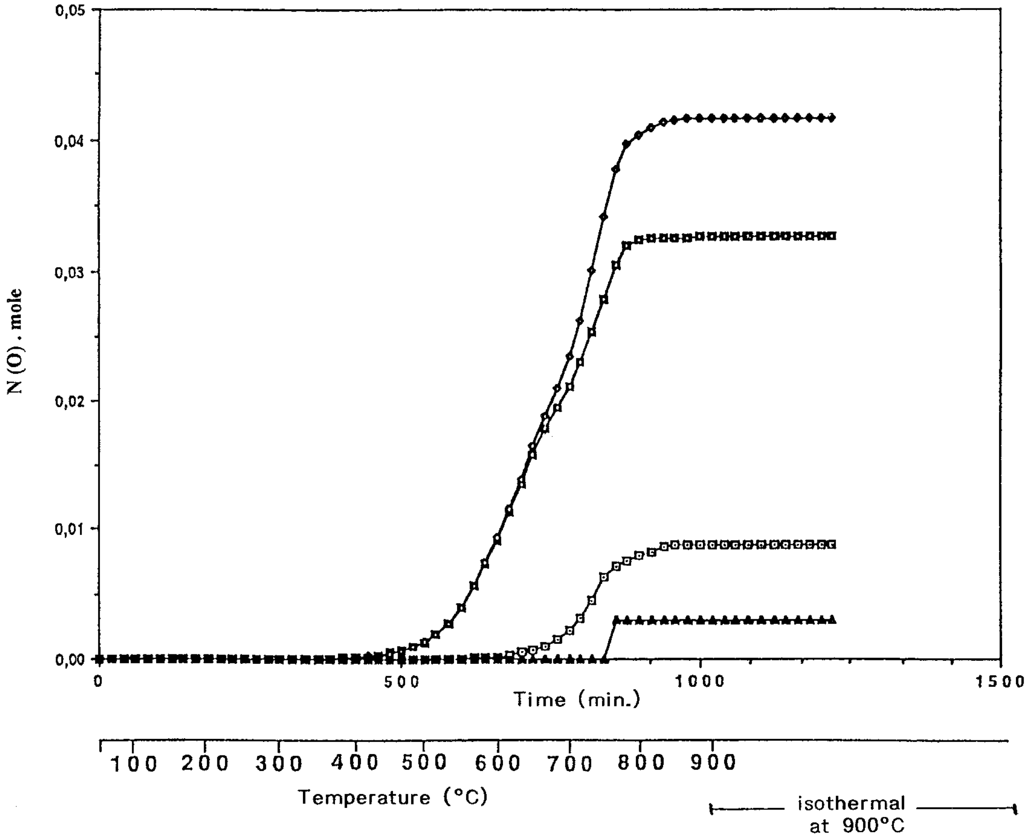

FIG. 16. Number of H_2O, CO, and CO_2 moles formed during temperature programmed carburization of WO_3 in 20% CH_4–H_2. ⊡ *N*(CO); □ *N*(H_2O); ◆ *N*(O total); ▲ *N*(CO_2) × 30.

carburization of *W* are very much dependent on the total pressure (hence on the pressure of H_2 for the first reaction and on that of CH_4 for the second reaction), since the temperature of the beginning of reduction by hydrogen shifts from about 300–400 to 700°C when hydrogen pressure is decreased from 1 atm to 1 Torr and the carburization of W metal starts at about 630 and 685°C when the percentage of CH_4 is equal to, respectively, 20 and 10% in CH_4–H_2 mixtures at atmospheric pressure.

The direct carburization of WO_3 by CH_4–H_2 has led to the conclusion that tungsten oxides cannot be directly carburized under the conditions studied here, but only W metal can be carburized. When W metal is formed at the surface of the incompletely reduced oxide, the phenomena observed are very different when the methane pressure is decreased, because of the competition between the diffusion of W metal from the surface into the bulk of the sample and its carburization at the surface. At high methane pressure (0.2 atm), W metal is carburized almost as soon as it is formed, as evidenced by *in situ* X-ray diffraction experiments during the temperature programmed carburization and by the amounts of oxygen (from the oxide) and of methane consumed as a function of the temperature. However, when the methane pressure is lower (0.02 atm or 1 Torr), the rate of W carburization is strongly decreased while that of W diffusion is not changed. Hence most of the W migrates into the solid before being carburized, and carburization occurs only at higher extents of reduction of W oxides into W metal. This results in a large shift of the temperature of the beginning of carburization. However, at such low methane pressures the consumption of CH_4 is very steep, indicating

TABLE 5

Ratio C/W in Sample WC1 and Ratio O/W (O consumed per W during reduction) as a Function of the Temperature of Reaction

Peak (CH_4 consumption)	Temperature (°C)	C/W	O/W
1	600–720	0.26	2.0
2	720–770	0.85	3.14
3	770–900	1.51	3.14

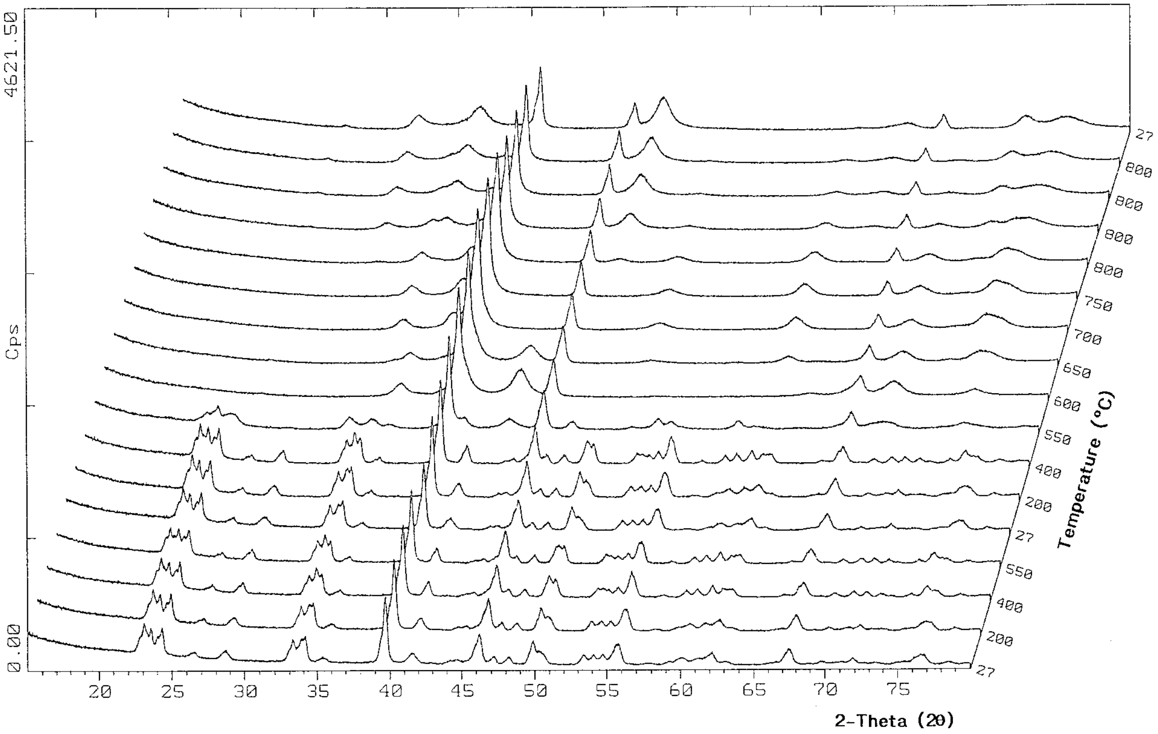

FIG. 17. X-ray diffraction patterns at different temperatures during *in situ* temperature programmed carburization of WO_3 (60°C h^{-1}, 20% CH_4–H_2).

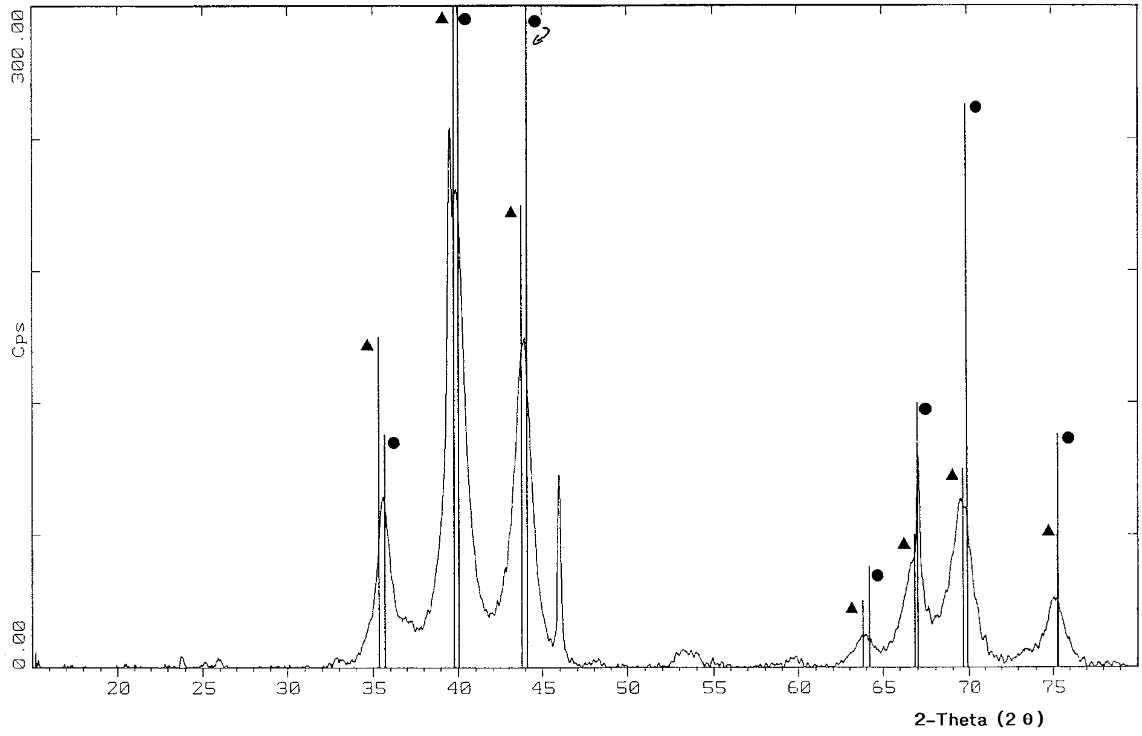

FIG. 18. X-ray diffraction pattern of WO_3 treated at 600°C in a mixture 20% CH_4–H_2. ▲ W_3O; ● W_3C.

TABLE 6

Results of the Temperature Programmed Carburization of Unreduced WO_3 at Various Pressures of 20% CH_4–H_2

$P_{CH_4} + P_{H_2}$ (atm)	Diluent	Reduction temperature (°C)			Carburization temperature (°C)	
		Beginning	First max.	Second max.	Beginning	Max.
1	None	300	630	750	600	650–720
0.3	Ar	500	640	780	760	810
0.1	Ar	540	800	~1000	870	980
6.6×10^{-3}	None	650	1000		1200	—

that carburization is very fast as soon as, due to the extended reduction of WO_3, some W metal becomes available at the surface of the solid.

For all the carbides obtained by carburization with a CH_4–H_2 mixture it has been shown that some free carbon is deposited at their surface and that some surface oxidation occurs during the passivation and the storage of the solids. However, their composition strongly depends on the temperature of carburization and on the CH_4 pressure, since the proportion of free carbon at the surface increases with methane pressure at a given temperature and with the temperature of carburization at a given CH_4 pressure. Only a small amount of carbon of pollution is observed after carburization at 650°C, but only free carbon can be observed by XPS after carburization at 900°C. However, the presence of free carbon can be advantageous, since the more free carbon at the surface the less the extent of oxidation of the W carbide surface, which shows that carbon of pollution protects W carbides from oxidation. Nevertheless, the presence of the oxide phases and of free carbon at the surface of carbides is obviously detrimental for their use in catalysis. Consequently some pretreatments for cleaning their surfaces will be necessary before catalytic experiments. These pretreatments will be described in a further paper.

APPENDIX I

Calculation of the Ratio X/N_0 Fraction of CH_4 Consumed Per Unit of Time during the Carburization of W Metal

The reactions that take place are

$$2W + CH_4 = W_2C + 2H_2$$
$$W + CH_4 = WC + 2H_2$$
$$W_2C + CH_4 = 2WC + 2H_2$$
$$CH_4 = C + 2H_2.$$

When 1 mol CH_4 disappears, 2 mol H_2 are formed.

N_0 denotes the number of moles CH_4 in the initial mixture per second,
X the number of moles CH_4 transformed per second, and
a the initial ratio of the molar fractions of H_2 and of CH_4.

The number of moles of CH_4 and H_2 flowing out of the reactor are

$$N_{CH_4} = N_0 - X \quad \text{and} \quad N_{H_2} = aN_0 + 2X.$$

One can calculate the partial pressure of CH_4

$$P_{CH_4} = \frac{P_T(N_0 - X)}{(a+1)N_0 + X} = \frac{(a+1)(P_{CH_4})_0(N_0 - X)}{(a+1)N_0 + X},$$

and the ratio X/N is

$$\frac{X}{N_0} = \frac{5[(P_{CH_4})_0 - P_{CH_4}]}{5(P_{CH_4})_0 - P_{CH_4}}.$$

Or, since P_{CH_4} is proportional to the area of the chromatographic peak corresponding to CH_4,

$$\frac{X}{N_0} = \frac{(a+1)[(S_{CH_4})_0 - S_{CH_4}]}{(a+1)(S_{CH_4})_0 + S_{CH_4}}.$$

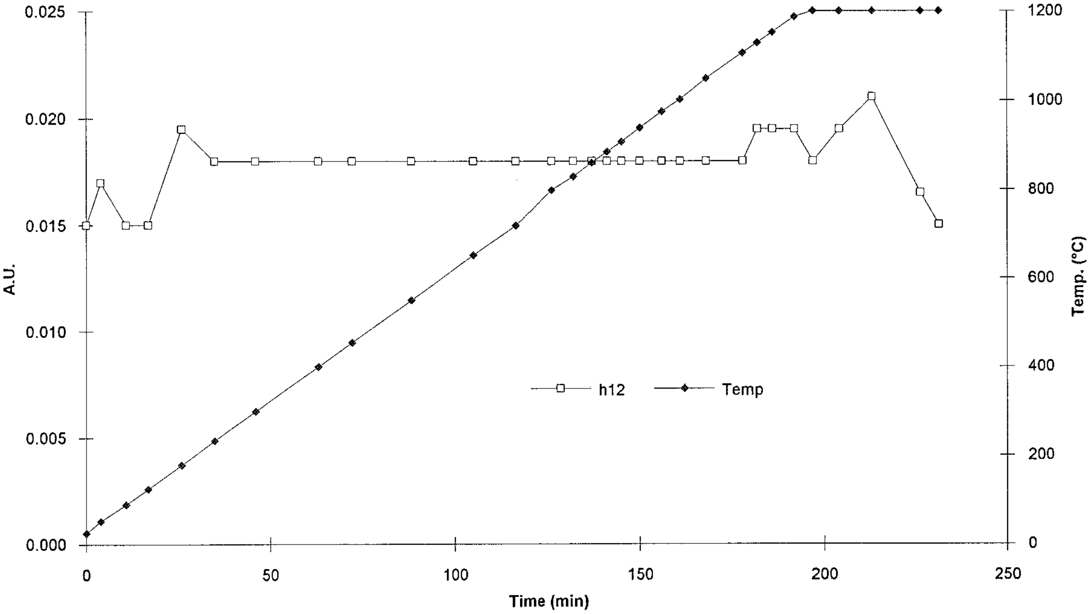

FIG. 19. Temperature programmed carburization of WO_3 in a mixture of 20% CH_4–D_2 at 5 Torr (360°C h^{-1}, 74 mg). Height of peak at mass 12 versus time.

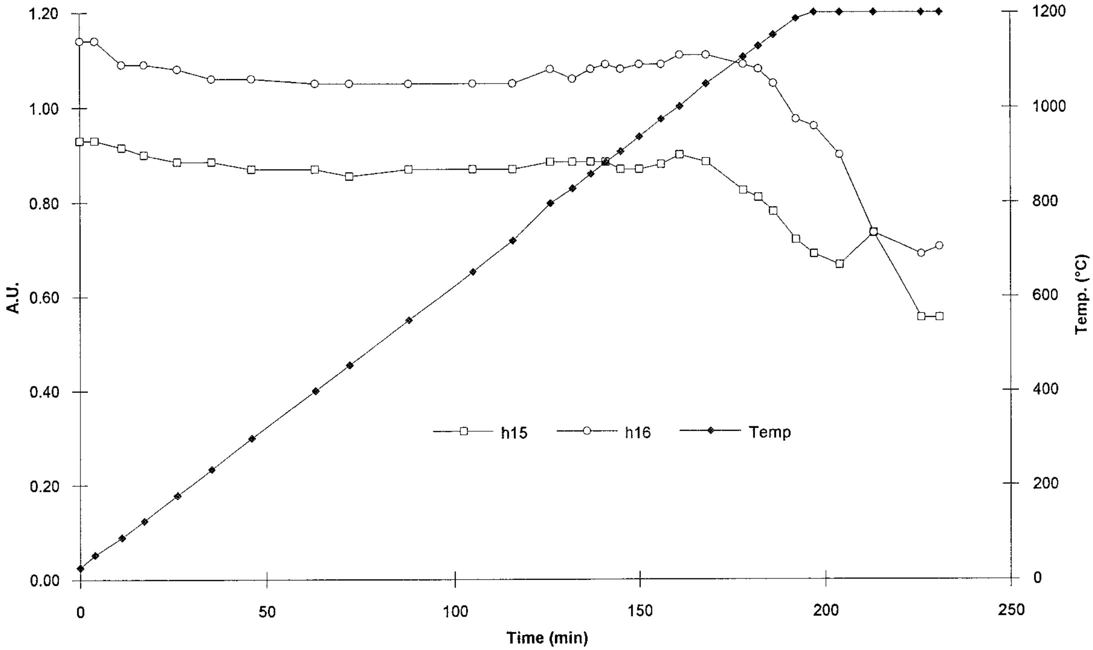

FIG. 20. Temperature programmed carburization of WO_3 in a mixture of 20% CH_4–D_2 at 5 Torr (360°C h^{-1}, 74 mg). Heights of peaks at mass 15 and 16 versus time.

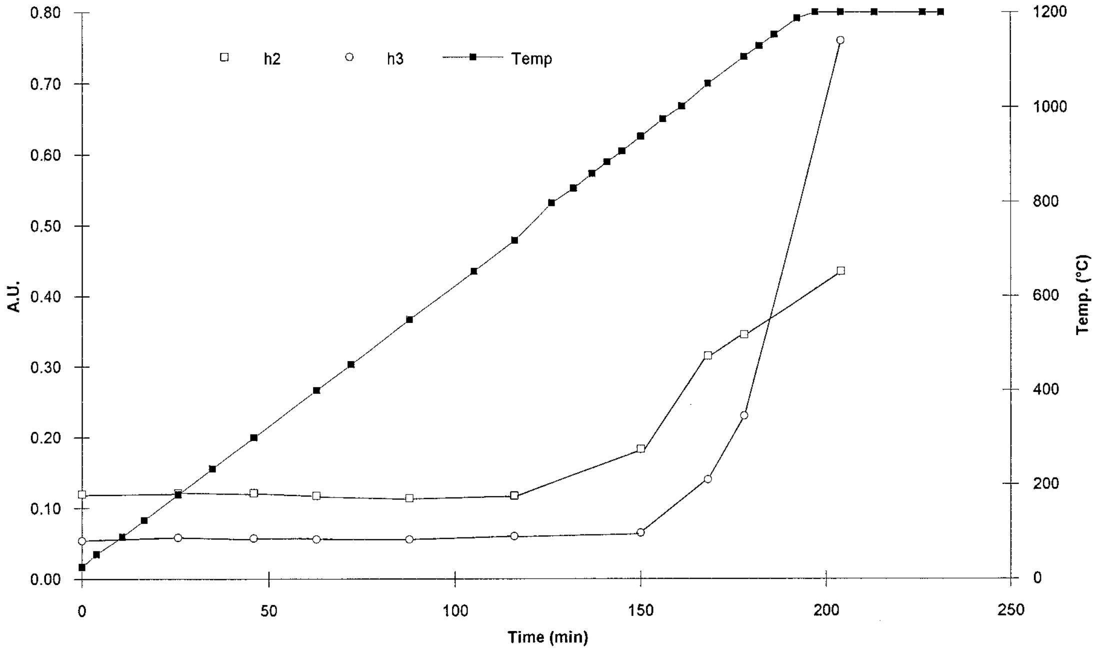

FIG. 21. Temperature programmed carburization of WO_3 in a mixture of 20% CH_4–D_2 at 5 Torr (360°C h^{-1}, 74 mg). Heights of peaks at mass 2 and 3 versus time.

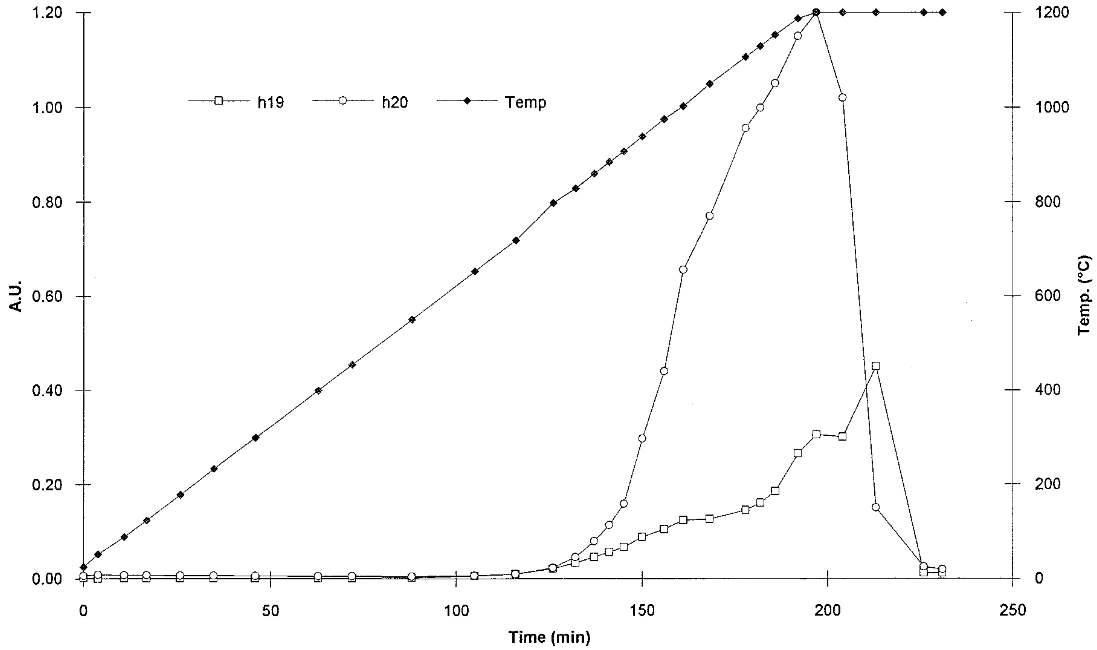

FIG. 22. Temperature programmed carburization of WO_3 in a mixture of 20% CH_4–D_2 at 5 Torr (360°C h^{-1}, 74 mg). Heights of peaks at mass 19 and 20 versus time.

TABLE 7

Carburization of WO_3 with 20% CH_4–D_2 at a Pressure of 5 Torr Mass Spectrometry Analysis

Temperature (°C)	h_{20} corr. (V)	h_{19} corr. (V)	h_{18} corr. (V)	h_{17} corr. (V)	$\frac{h_{17}\text{ corr.}}{h_{19}\text{ corr.}}$	$\frac{h_{17}\text{ corr.}}{h_{19}\text{ corr.} + h_{20}\text{ corr.}}$
652	0.0013	0.0036	0.0024	0.0009	0.25	0.49
718	0.0046	0.0081	0.0057	0.0012	0.15	0.45
798	0.0175	0.0195	0.0129	0.0027	0.14	0.35
829	0.0405	0.0317	0.0216	0.0035	0.11	0.30
860	0.0740	0.0442	0.0316	0.0055	0.12	0.27
884	0.1090	0.0547	0.0421	0.0060	0.11	0.26
907	0.1540	0.0652	0.0549	0.0075	0.12	0.25
938	0.2920	0.0867	0.0916	0.0110	0.13	0.24
975	0.4350	0.1032	0.1416	0.0150	0.14	0.26
1002	0.6500	0.1212	0.1816	0.0225	0.19	0.24
1049	0.7650	0.1242	0.2106	0.0375	0.30	0.24
1106	0.9500	0.1432	0.2776	0.1225	0.85	0.25
1129	0.9940	0.1582	0.3076	0.1465	0.93	0.27
1152	1.0450	0.1832	0.3406	0.1715	0.94	0.28
1187	1.145	0.2632	0.4376	0.1965	0.75	0.31
1200	1.195	0.3032	0.4576	0.1965	0.65	0.30
1200	1,0150	0.2982	0.4276	0.1815	0.61	0.32
1200	0.1450	0.0432	0.0626	0.0315	0.73	0.33
1200	0.0205	0.0102	0.0156	0.0255	2.5	0.51

APPENDIX II

Calculation of the Ratios X/N_0, Y/N_0, Z/N_0, and N_{H_2O}/N_0 (X, Y, Z, N_{H_2O} = Number of Moles CH_4 Consumed Per Second for Carburization (X), for CO Formation (Y), for CO_2 Formation (Z), and Number of Moles H_2O Formed Per Second) during the Carburization of WO_3

The reactions taking place are

$$H_2 + \text{“O”} = H_2O$$

$$WO_3 + CH_4 = WO_2 + CO + 2H_2$$

$$WO_2 + 2CH_4 = W + 2CO + 2H_2$$

$$WO_2 + CH_4 = W + CO_2 + 2H_2$$

$$CH_4 + H_2O = CO + 3H_2$$

$$CH_4 + 2H_2O = CO_2 + 4H_2$$

and the reactions of carburization (see Appendix I) and/or any combination of these equations.

One can see that when 1 mol of CO or CO_2 is formed there is an increase of 2 mol in the gas phase; when 1 mol of CH_4 is consumed for carburization or carbon deposition, there is an increase of 1 mol in the gas phase, and the disappearance of 1 mol of H_2 does not change the number of mol in the gas phase.

Hence, $\sum N = (a + 1)N_0 + X + 2Y + 2Z$ using the same meaning for a and N_0 as in Appendix I.

The various partial pressures are

$$P_{CH_4} = \frac{P_T(N_0 - X - Y - Z)}{\sum N}$$

$$P_{CO} = P_T \frac{Y}{\sum N} \quad P_{CO_2} = P_T \frac{Z}{\sum N}$$

and

$$P_{H_2O} = P_T \frac{N_{H_2O}}{\sum N}$$

since

$$P_T = (a + 1)(P_{CH_4})_0.$$

One can easily calculate

$$\frac{X}{N_0} = \frac{(a+1)[(P_{CH_4})_0 - P_{CH_4}] - (a+3)[P_{CO} + P_{CO_2}]}{(a+1)(P_{CH_4})_0 + P_{CH_4} - P_{CO} - P_{CO_2}}$$

$$\frac{Y}{N_0} = \frac{(a+2)P_{CO}}{(a+1)(P_{CH_4})_0 + P_{CH_4} - P_{CO} - P_{CO_2}}$$

$$\frac{Z}{N_0} = \frac{(a+2)P_{CO_2}}{(a+1)(P_{CH_4})_0 + P_{CH_4} - P_{CO} - P_{CO_2}}$$

$$\frac{N_{H_2O}}{N_0} = \frac{(a+2)P_{H_2O}}{(a+1)(P_{CH_4})_0 + P_{CH_4} - P_{CO}P_{CO_2}}.$$

P_{CH_4}, P_{CO}, P_{CO_2}, and P_{H_2O} are proportional to the areas of the chromatographic peaks corresponding to, respectively, CH_4, CO, CO_2, and H_2O, taking into account the molar response factors of the TCD.

ACKNOWLEDGMENTS

This work was supported by a Stimulation Contract ST2J-0467-C(TT) from the EEC.

REFERENCES

1. Toth, L. E., "Transition Metal Carbides and Nitrides." Academic Press, New York, 1971.
2. Levy, R. B., and Boudart, M., *Science* **181,** 547 (1973).
3. Levy, R. B., *Adv. Mater. Catal.* 101 (1977).
4. Oyama, S. T., and Haller, G. L., *Catal. Spec. Per. Rep.* **5,** 333 (1982).
5. Leclercq, L., *in* "Proceedings of the Nato Advanced Study Institute, Lille, France, 1982" (J. P. Bonnelle, B. Delmon, and E. Derouane, Eds.), p. 433. Reidel, Dordrecht, 1983.
6. Ribeiro, F. H., Boudart, M., Dalla Betta, R. A., and Iglesia, E., *J. Catal.* **130,** 498 (1991).
7. Iglesia, E., Baumgartner, J. E., Ribeiro, R. H., and Boudart, M., *J. Catal.* **131,** 137 (1991).
8. Keller, V., Cheval, M., Vayer, M., Ducros, R., and Maire, G., *Catal. Lett.* **10,** 137 (1991).
9. Miles, R., *J. Chem. Tech. Biotechnol.* **30,** 35 (1980).
10. Nakazawa, N., and Okamoto, H., *Appl. Surf. Sci.* **24,** 75 (1985).
11. Leclercq, L., Provost, M., Pastor, H., Grimblot, J., Hardy, A. M., Gengembre, L., and Leclercq, G., *J. Catal.* **117,** 371 (1989).
12. Boudart, M., Oyama, S. T., and Volpe, L., U.S. Patent 4, 515, 763, 1985.
13. Volpe, L., and Boudart, M., *J. Solid State Chem.* **59,** 332 and 348 (1985).
14. Lee, J. S., Oyama, S. J., and Boudart, M., *J. Catal.* **106,** 125 (1987).
15. Leclercq, L., Imura, K., Yoshida, S., Barbee, T., and Boudart, M., *in* "Preparation of Catalysts II", (B. Delmon, P. Grange, and G. Poncelet, Eds.), p. 627 Elsevier, Amsterdam, 1978.
16. Lemaître, J., Vidick, B., and Delmon, B., *J. Catal.* **99,** 415 (1986).
17. Vidick, B., Lemaître, J., and Delmon, B., *J. Catal.* **99,** 428 (1986).
18. Boudart, M., and Leclercq, L., U.S. Patent 4, 271, 041, 1981.
19. Boudart, M., Oyama, S. T., and Leclercq, L., "Proceedings 7th International Congress on Catalysis, Tokyo, 1980" (T. Seiyama and K. Tanabe, Eds.), p. 578. Elsevier, Amsterdam, 1981.
20. Laine, R. M., and Hirschon, A., *in* "Better Ceramics Through Chemistry II" (C. J. Brinker, D. E. Clark, and D. R. Ulrich, Eds.). Materials Research, New York, 1984.
21. Giraudon, J. M., Leclercq, L., Leclercq, G., Löfberg, A., Frennet, A., *J. Mater. Sci.* **28,** 2449 (1993).
22. Ledoux, M. J., Pham Huu, C., Marin, S., Guille, J., and Weibel, M., *C. R. Acad. Sci. Ser. II* 707 (1990).
23. Ledoux, M. J., Pham Huu, C., Guille, J., and Dunlop, H., *J. Catal.* **134,** 383 (1992).
24. Mooney, W., Chiola, V., Hoffman, C. W. W., and Vanderpool, C. D., *J. Electro. Chem. Soc.* **109,** 1179 (1962).
25. Leclercq, G., Leclercq, L., and Maurel, R., *J. Catal.* **5,** 87 (1977).
26. Kaganer, M. G., *Zhur. Fiz. Khim.* **33,** 2202 (1959).
27. Delaunois, Y., Frennet, A., and Lienard, G., *J. Chim. Phys.* **63,** 906 (1966).
28. (a) Tilley, R. D. J., "Defect Crystal Chemistry and its Applications," Blackie Glasgow/London, 1987; (b) Hansen, M., "Constitution of Binary Alloys" p. 1076. McGraw–Hill, New York, 1958.
29. Vermaire, D. C., and Van Berge, P. C., *J. Catal.* **116,** 309 (1989).
30. Grünert, W., Shpiro, E. S., Feldhaus, R., Anders, K., Antoshin, G. V., and Minachev, K. M., *J. Catal.* **107,** 522 (1987).
31. Barin, I., and Knacke, O., "Thermochemical Properties of Inorganic Substances." Springer Verlag, Berlin, 1973.
32. Lee, J. S., Locatelli, S., Oyama, S. T., and Boudart, M., *J. Catal.* **125,** 157 (1990).
33. Rodero, A., Ph.D. Thesis, University of South Florida, 1976.
34. Jama, C., Dessaux, O., Goudmand, P., Gengembre, L., and Grimblot, J., *Surf. Interface Anal.* **18,** 751 (1992).
35. Bonzel, H. P., and Krebs, H. J., *Surf. Sci.* **91,** 199 (1980).
36. Bou, M., Martin, J. M., Lemogne, T., and Vovelle, L., *Appl. Surf. Sci.* **47,** 149 (1991).
37. Dianis, W. P., and Lester, J. E., *Anal. Chem.* **45,** 1416 (1973).
38. Blanchard, L., Grimblot, J., and Bonnelle, J. P., *J. Catal.* **98,** 229 (1986).
39. Grimblot, J., Payen, E., and Bonnelle, J. P., "Proceedings of the Fourth Climax Molybdenum International Conference Sponsored (Ann Arbor, Michigan)" (H. F. Barry and P. C. H. Mitchell, Eds.), p. 261. University of Reading, England, 1982.
40. Rostrup-Neilsen, J. R., *J. Catal.* **31,** 173 (1973).
41. Vitidsant, T., Laguerie, C., Gilot, B., and Damronglerd, S., *Bull. Soc. Chim. France* 194 (1989).